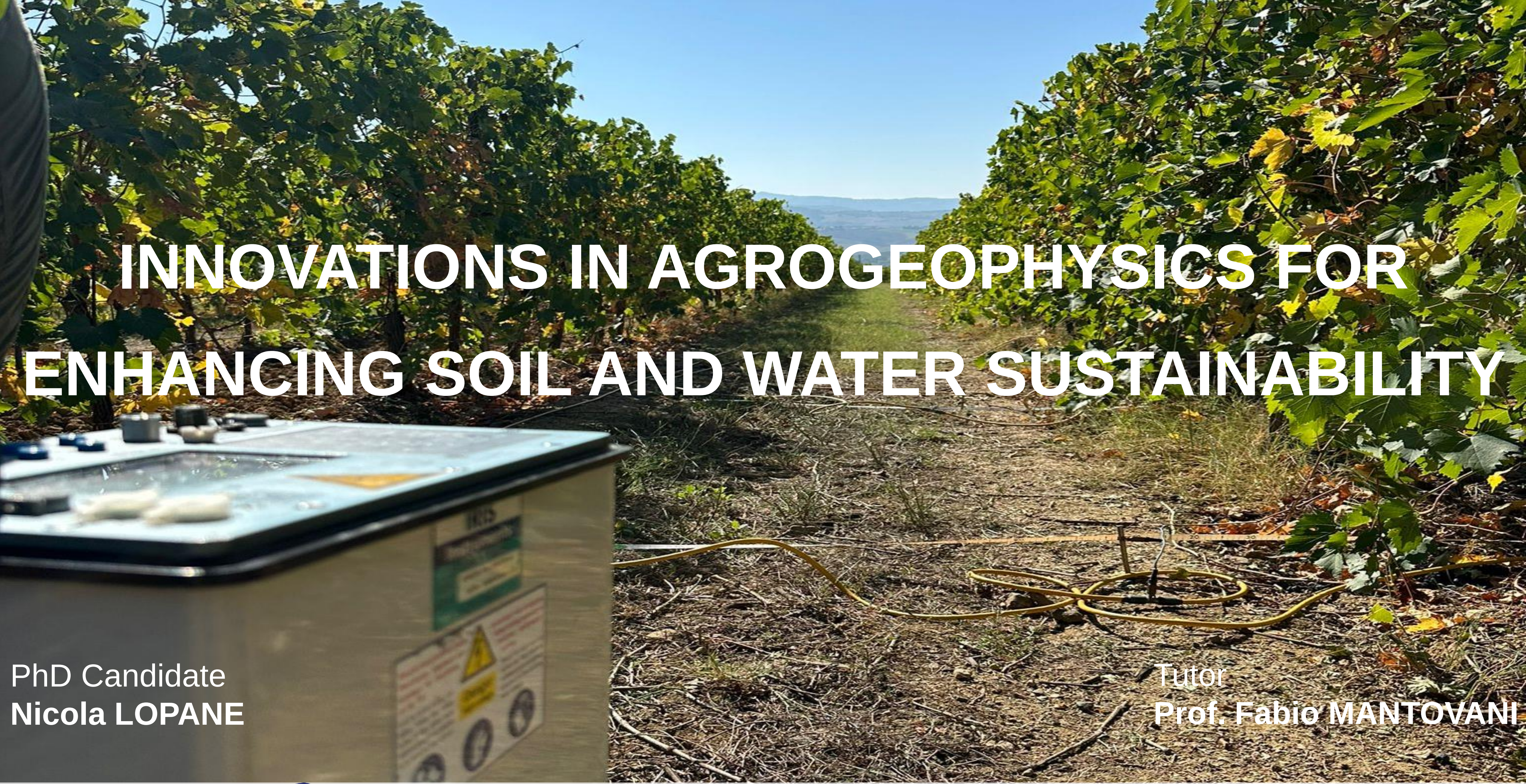

INNOVATIONS IN AGROGEOPHYSICS FOR ENHANCING SOIL AND WATER SUSTAINABILITY

PhD Candidate
Nicola LOPANE

Tutor
Prof. Fabio MANTOVANI

Università degli Studi di Ferrara
INFN

Ph.D. in Physics – Cycle XXXVII
Ferrara - 29 April 2025

GEOexplorer
Laboratory for Nuclear Technologies Applied to the Environment

My research motivations

Over **70%** of agronomic decisions in Italy still rely on empirical knowledge, while less than **15%** of farms use advanced data-driven methods

(Vecchio, Y. et al. (2020). Adoption of Precision Farming Tools: The Case of Italian Farmers. Agronomy, 10(1): 18. (MDPI))

Gap in the adoption of quantitative methods for monitoring and managing field conditions

Agriculture generates **420 B€/year** and employs 22 million people, in addition climate events have cost Italian agriculture over **14 B€** in 10 years

(Hannah Ritchie and Ma. Roser (2019), ‘Land Use’, Our World in Data)

Resource-use efficiency directly supports income, employment, and economic resilience

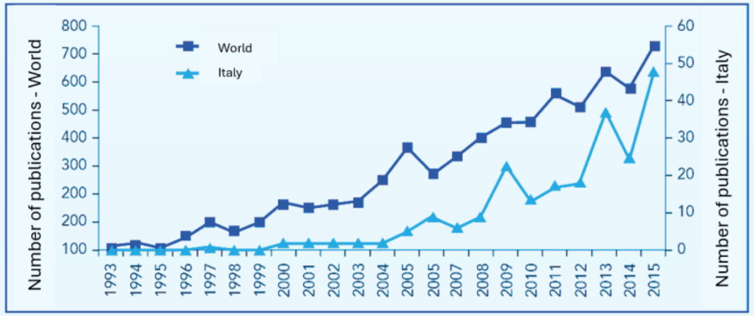

Casa, R. (2016). Agricoltura di precisione, metodi e tecnologie per migliorare l’efficienza e la sostenibilità dei sistemi colturali. Edagricole-Edizioni Agricole di New Business Media Srl

From around **30** publications pre-2010, precision agriculture surged to over **1,100** articles annually by 2020, driven by digital and automated technologies

(*Rejeb, A. et al. (2024). Precision Agriculture: A Bibliometric Analysis and Research Agenda. Smart Agricultural Technology 9: 100684*)

Developing innovative methods on real data to support sustainable management in agricultural contexts

Keywords of my research

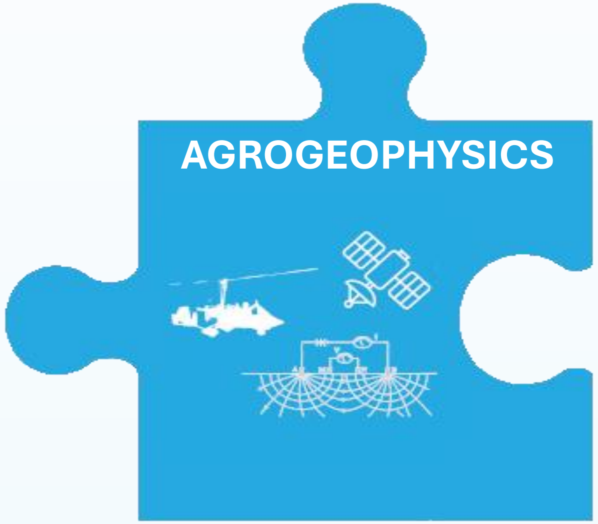

Near-surface **geophysics** applies non-invasive methods to assess **soil** and **crop** properties, linking geosciences with agriculture to enhance field characterization and management for improved crop production and resource efficiency

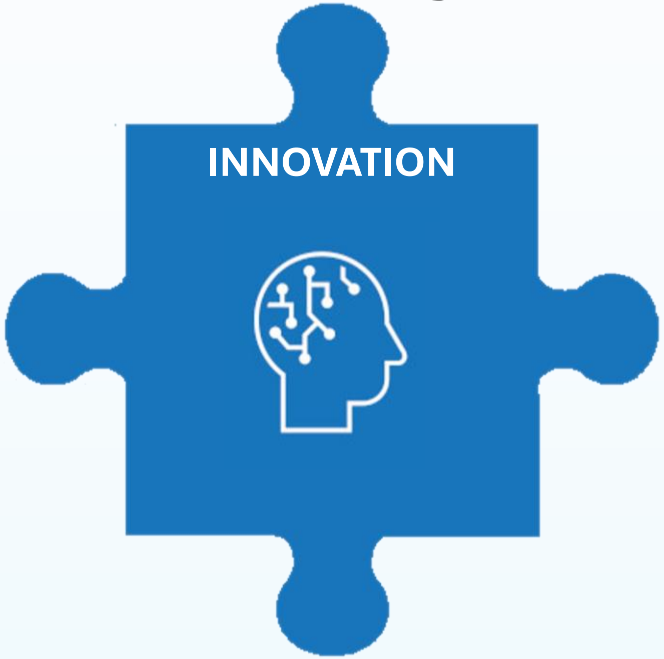

Application of new or existing knowledge to **develop** or **improve** products, processes, or methods seeks to create added value, enhance performance, and generate new insights through original and practical solutions

Fulfilling **present needs** without depleting **future resources** by balancing human demands with natural limits, ensuring the conservation and stability of ecosystems to support the well-being and resilience of future generations

Advancements in agrogeophysics

Leveraging technological approaches and physical methods to improve soil and water sustainability

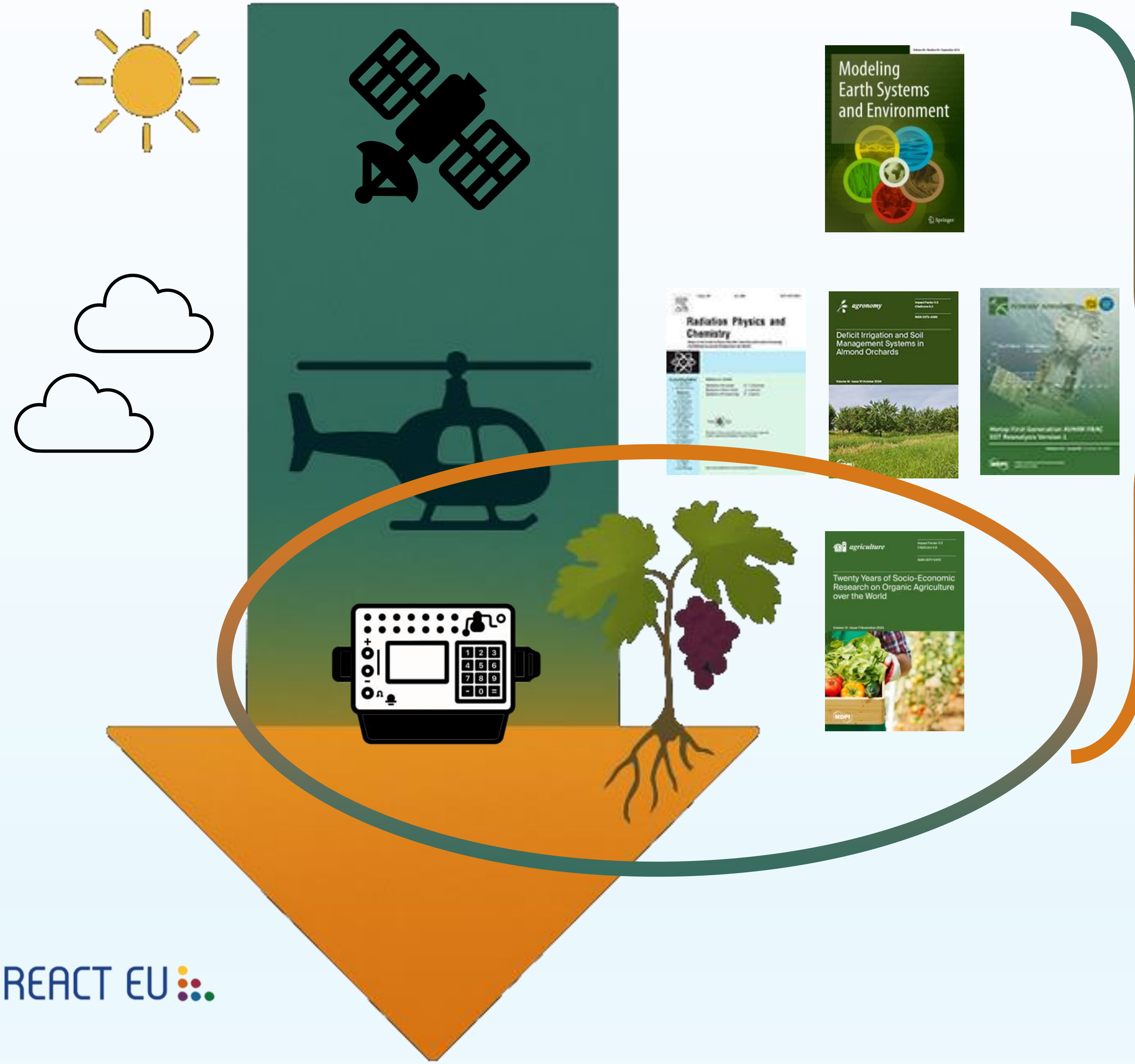

My PhD thesis

UNIONE EUROPEA
Fondo Sociale Europeo
Ministero dell'Università e della Ricerca
PON RICERCA E INNOVAZIONE
REACT EU

Geoelectric joint inversion for 3D imaging of vineyard ground *

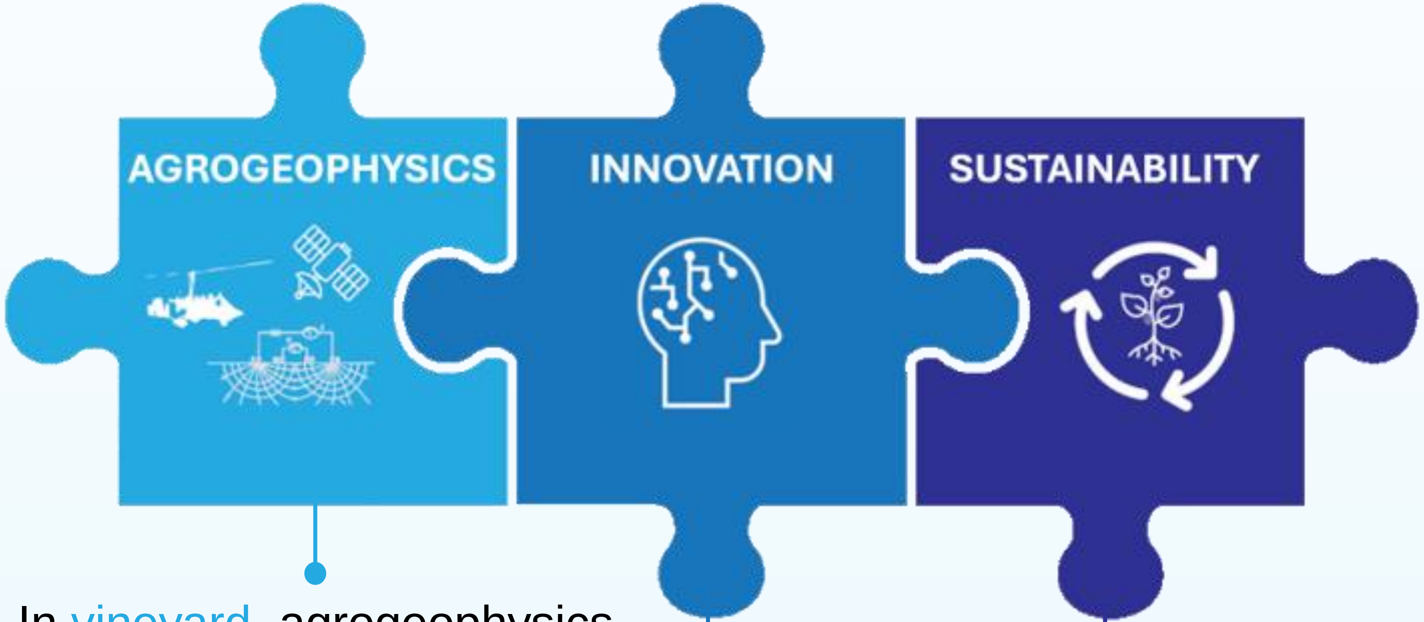

In vineyard, agrogeophysics made it possible to map vine root systems and soil conditions in 3D

By identifying how water moves underground, the model helps manage irrigation precisely

Joint inversion of CCR and GCR, a new approach that improves subsurface imaging in vineyards

* Lopane, N., Albéri, M., Barbagli, A., Chiarelli, E., Colonna, T., Gallorini, F., ... & Strati, V. (2024). Geoelectric Joint Inversion for 3D Imaging of Vineyard Ground. *Agronomy*, *14*(11), 2489.

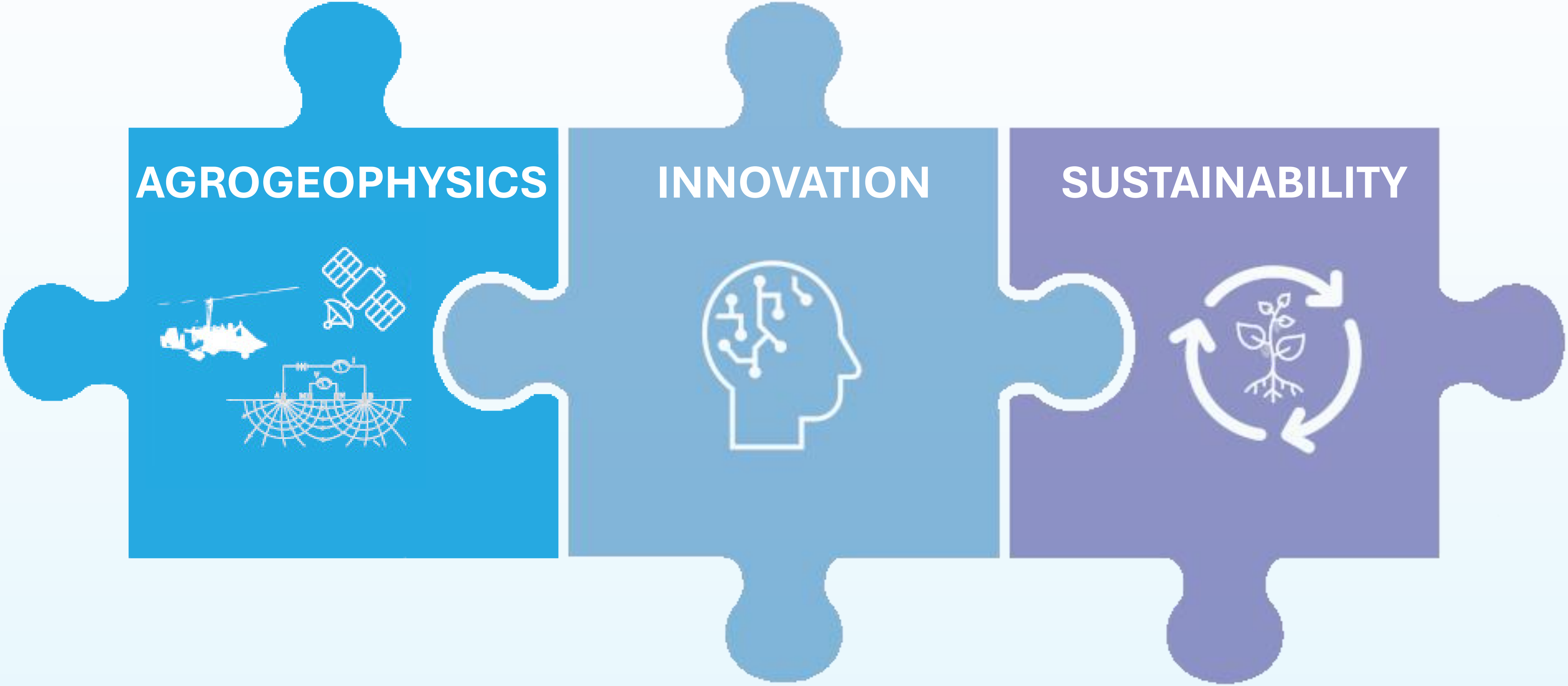
AGROGEOPHYSICS
INNOVATION
SUSTAINABILITY

Location, soil texture and peculiar problem

"**Il Poggione**" estate, Tuscany (Italy)
Brunello di Montalcino

Loamy texture

31.8% sand
34.9% silt
33.3% clay

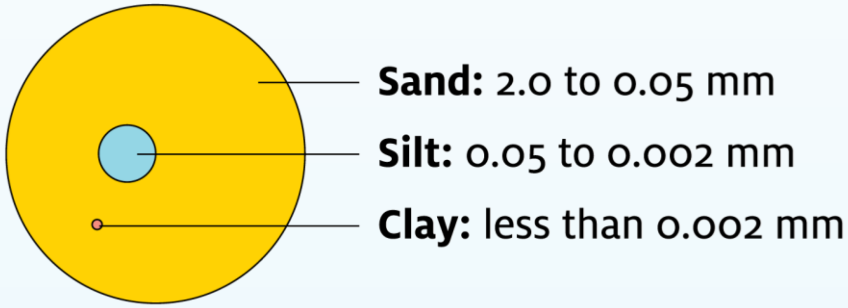

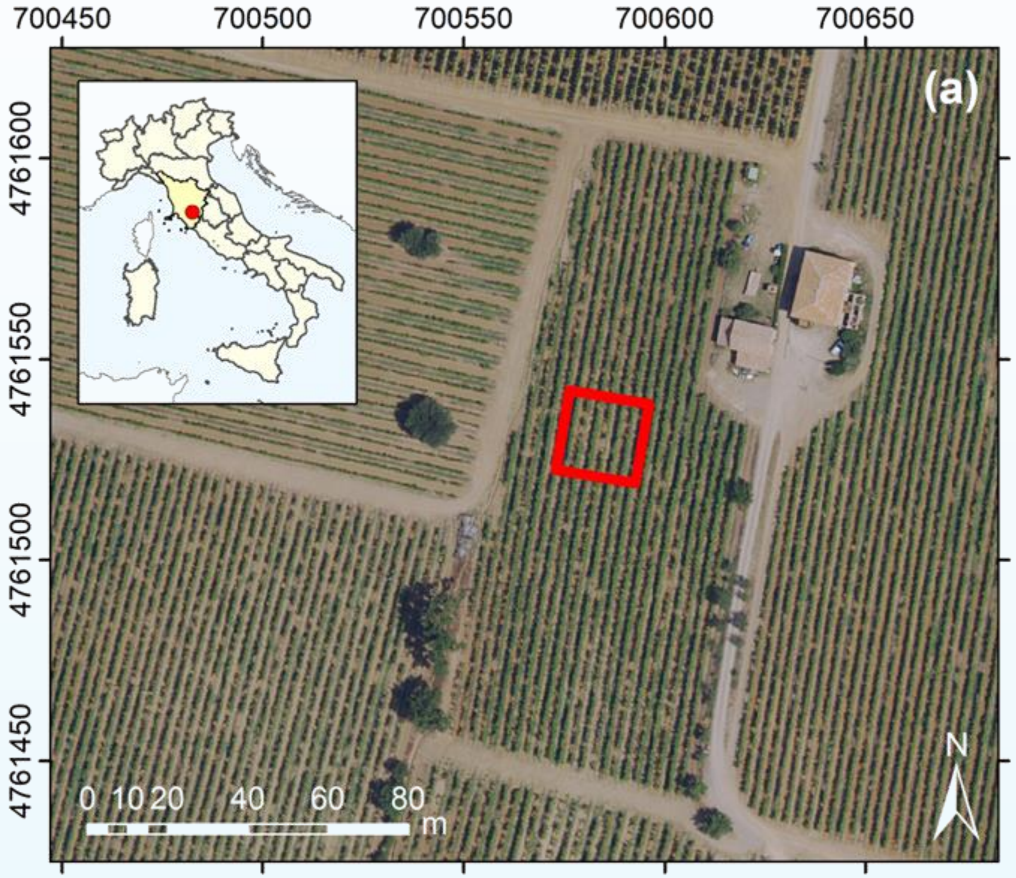

The vineyard faces a significant irrigation challenge, particularly in identifying and utilizing available water resources, as required for efficient relief irrigation under **Law 238/2016**

Grapevine root architecture: depth and structure

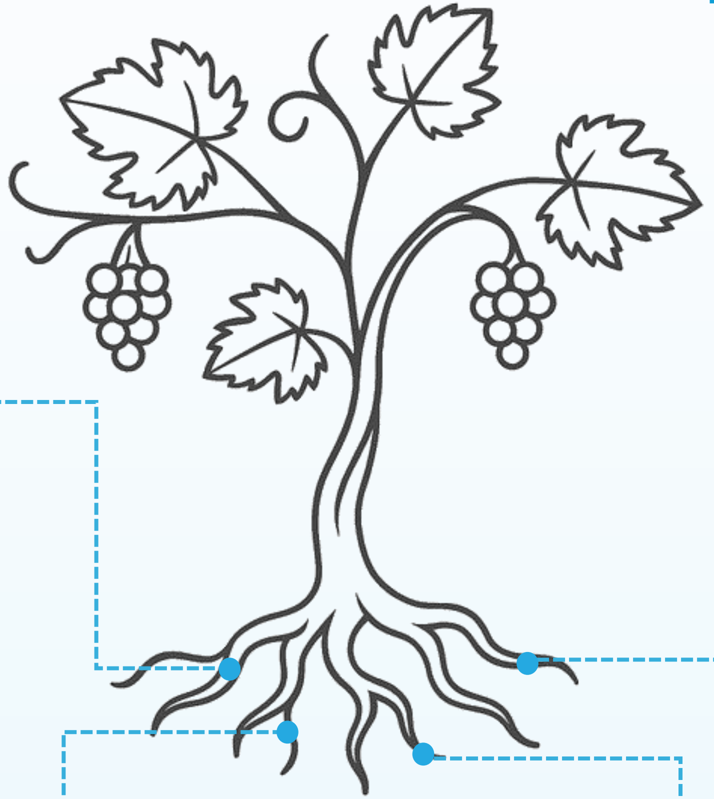

Root structure

- Framework roots: **6–100 mm Ø**
- Permanent roots: **2–6 mm Ø**
- Lateral roots**:** respond to **water** and **nutrient** zones

Percentage root concentration

- ~63% in the top **60 cm**
- ~80% within the top **100 cm**

Maximum root penetration

Soil structure affects maximal root depth, requiring **favorable conditions** like the absence of compacted layers and gravel-rich horizons

Depth drivers

Determined mainly by **soil properties**:

- Texture
- Bulk density
- Water content

Resistivity

Galvanic Contact Resistivity (GCR)

The **Syscal Pro** uses 96 electrodes and a 10-channel system to inject 1359 currents (~ 150 mA) into the soil, measuring **resistivity** with a transmitter and resistivimeter, powered by a 12 V external battery

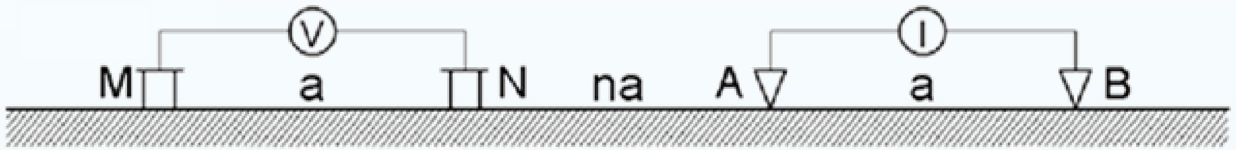

Spatial layout: **16 x 18 m**

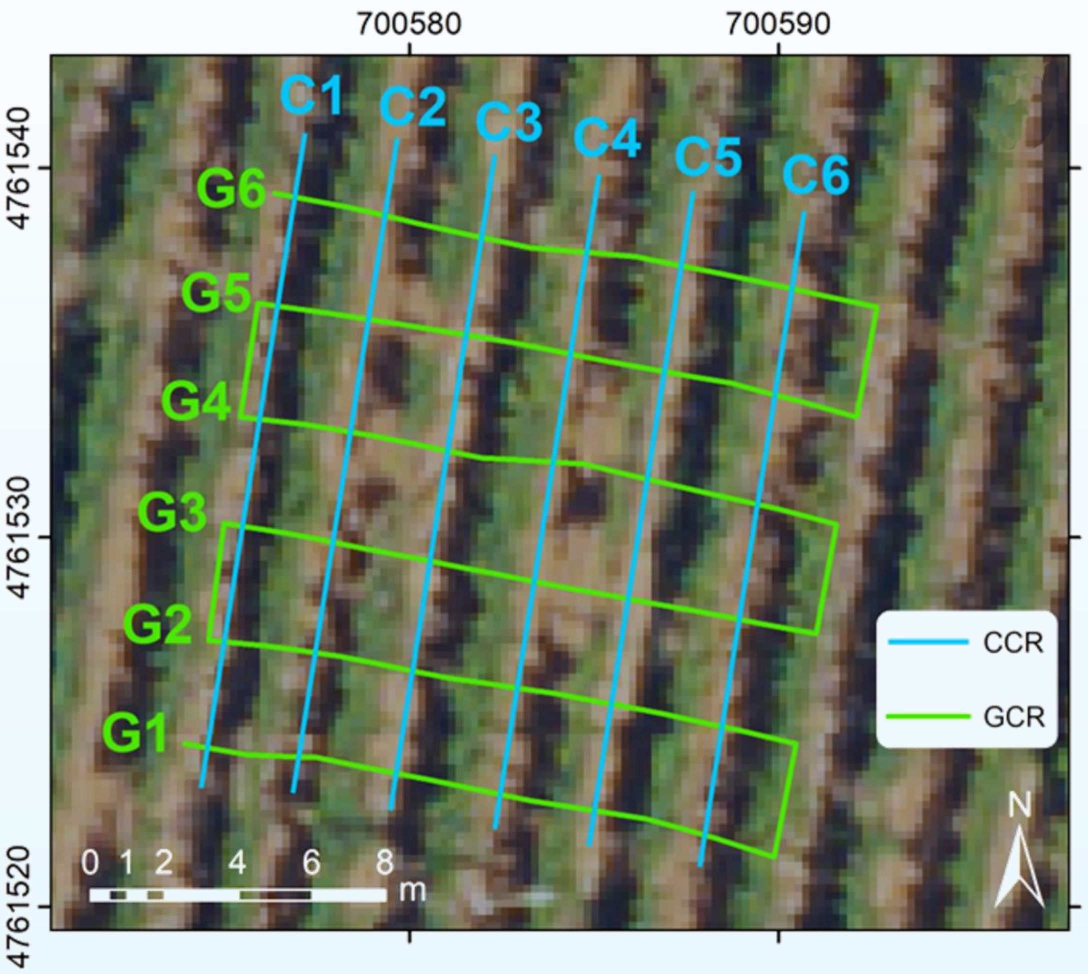

Strengths

- Depth range: up to 5 m
- High subsurface resistivity accuracy

Weaknesses

- Soil contact via electrodes
- Setup is labor-intensive

Capacitively-Coupled Resistivity (CCR)

The **OhmMapper** uses ungrounded transmitter and receiver dipoles, a tow cable, and control unit to inject 16.5 kHz AC (up to 12 V, 16 mA), recording **resistivity** data at 2 Hz

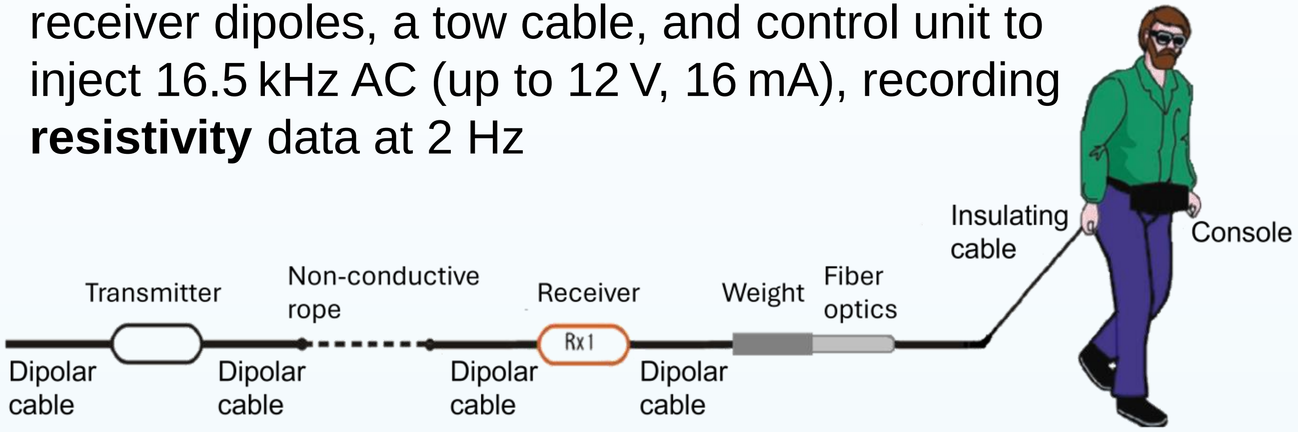

Spatial layout: **16 x 18 m**

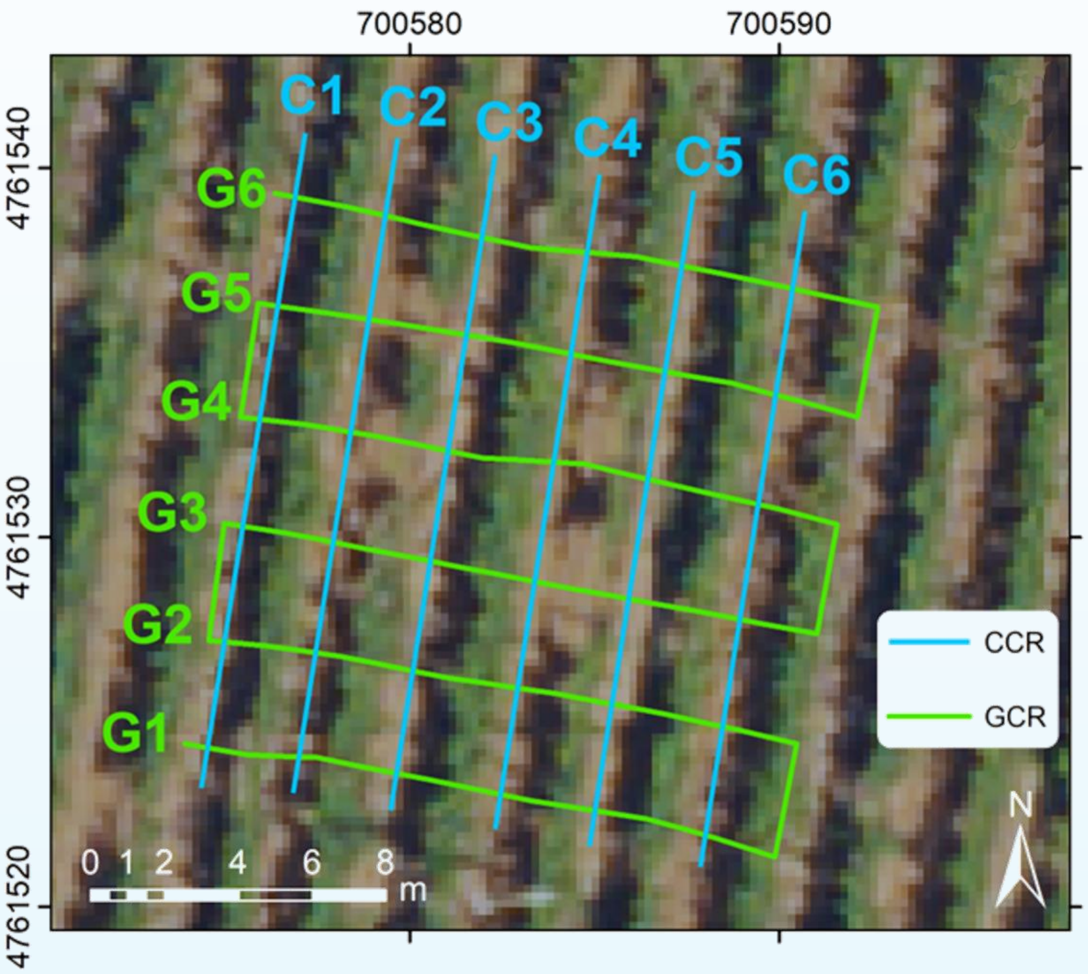

Strengths

- Non-invasive
- High resolution shallowest layers

Weaknesses

- Limited depth penetration
- Lower accuracy in deeper layers

Parameters for geoelectrical surveys

	GCR		CCR
Electrode distance (m)	1	Cord length (m)	1.25 – 5 – 10
Max depth (m)	~ 5.5	Max depth (m)	~ 3.5
Spread length (m)	16	Run length (m)	18
Number of spreads	6	Number of runs	6
Spread distance (m)	3	Run distance (m)	2.7
Method	Dipole-Dipole	Method	Dipole-Dipole
Acquisition dur (h)	0:48	Acquisition dur (h)	2:17
Min V/I (Ω)	$1.45 \cdot 10^{-5}$	Min V/I (Ω)	$1.90 \cdot 10^{-5}$
Max V/I (Ω)	3.01	Max V/I (Ω)	1.52
Max n + 1a (m)	20	Max n + 1a (m)	7
N° measurements acquired	5049	N° measurements acquired	384

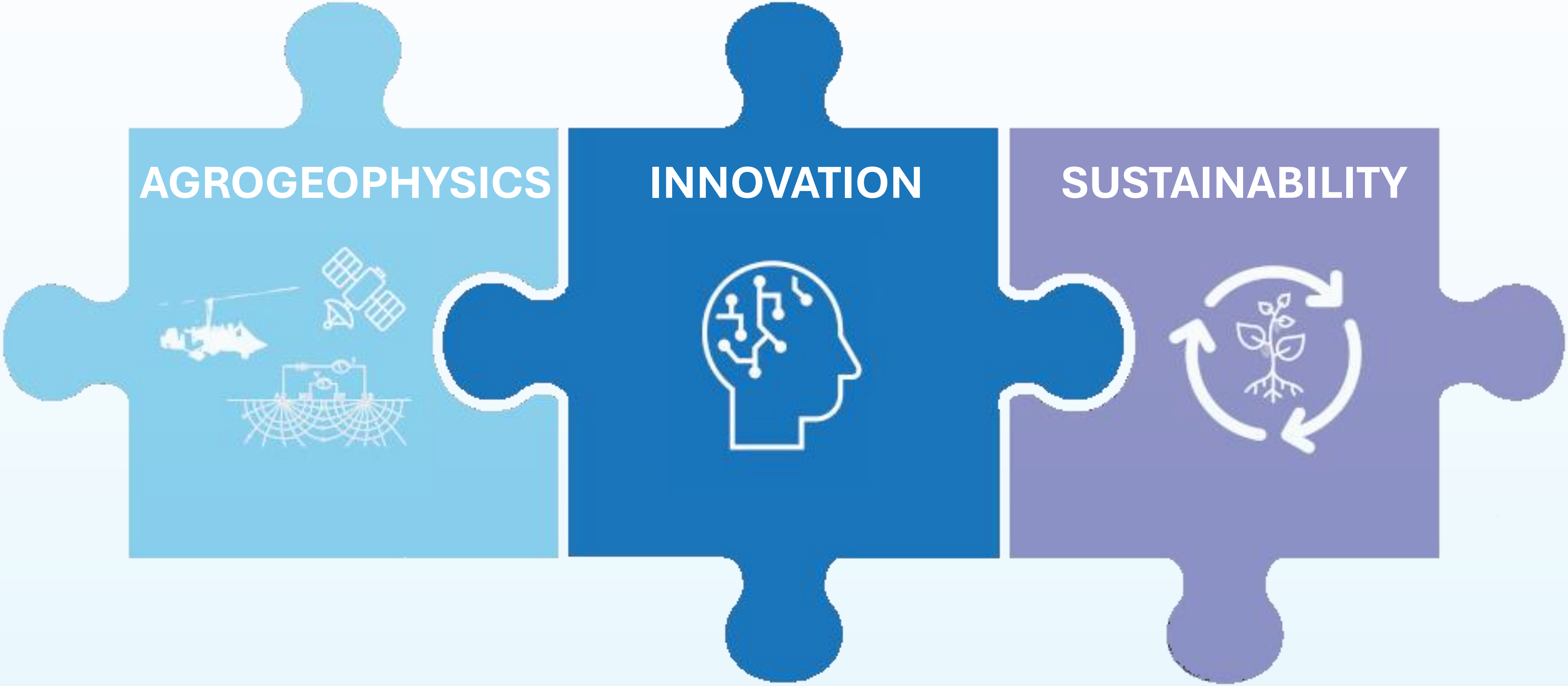
AGROGEOPHYSICS
INNOVATION
SUSTAINABILITY

Joint inversion in geophysics

Joint inversion was first proposed by Vozoff & Jupp (1975) to address ambiguities in single-method inversions by combining different geophysical data types

Methodology

Process

- Integrates multiple datasets (e.g. seismic, resistivity) to model complex subsurface structures
- Coupling techniques to merge data types effectively

Coupling Types

- Direct coupling: links physical properties directly
- Cross-gradient coupling: aligns structural patterns without assuming direct relationships

Key advantages

Enhanced Resolution

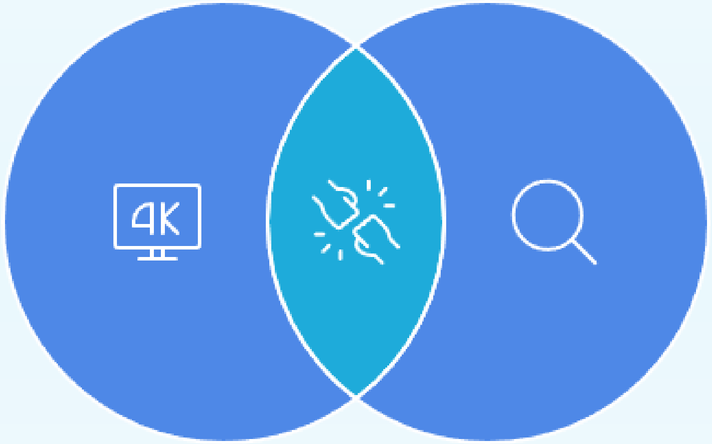

Reduced Ambiguity

Geoelectrical joint inversion

Idea

Both GCR and CCR measure subsurface electrical resistivity (in Ω·*m*), based on **Ohm's law**:

$$\rho_a = k\,\frac{V}{I}$$

where V is the voltage (in *V*), I is the current (in *A*), k is the geometric factor (in m).

- **GCR**: Measures voltage (V) via DC through electrodes, with potential Φ (in *V*) given by

$$\Phi = \frac{\rho I}{2\pi r}$$

- **CCR**: Uses capacitive coupling, with transfer impedance Z (in Ω)

$$Z = \frac{1}{i\omega C_O}(1 - K_{ES}\alpha)$$

Novelties

- First-time joint inversion combining two geophysical methods measuring the **same physical quantity (electrical resistivity)**, instead of different ones (e.g., seismic and electric).
- First application of this methodology in **agrogeophysics**, providing 3D resistivity imaging of a vineyard.

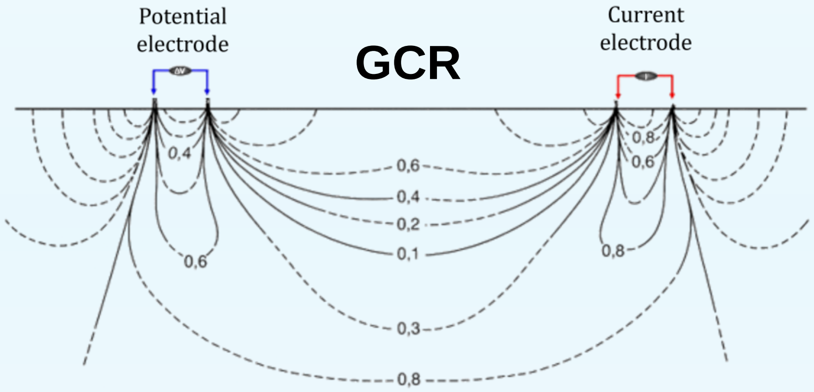

Expected benefits

- **Stronger constraints**: using GCR and CCR together strengthens the inversion by constraining the model with the same property, reducing non-uniqueness.
- **Sharper resolution**: combining GCR and CCR data produced a 3D model with 20.21 data/m³, improving resolution.
- **Multi-scale sensitivity**: combining GCR and CCR improves depth sensitivity: CCR provides surface resolution, GCR enables deeper characterization.

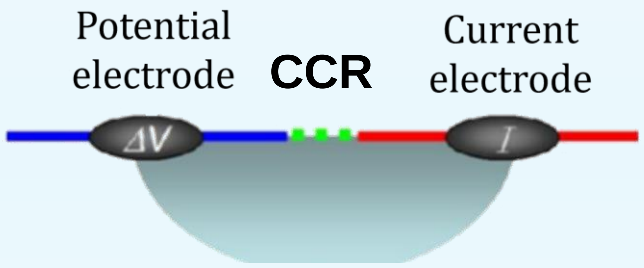

Geoelectrical joint inversion framework

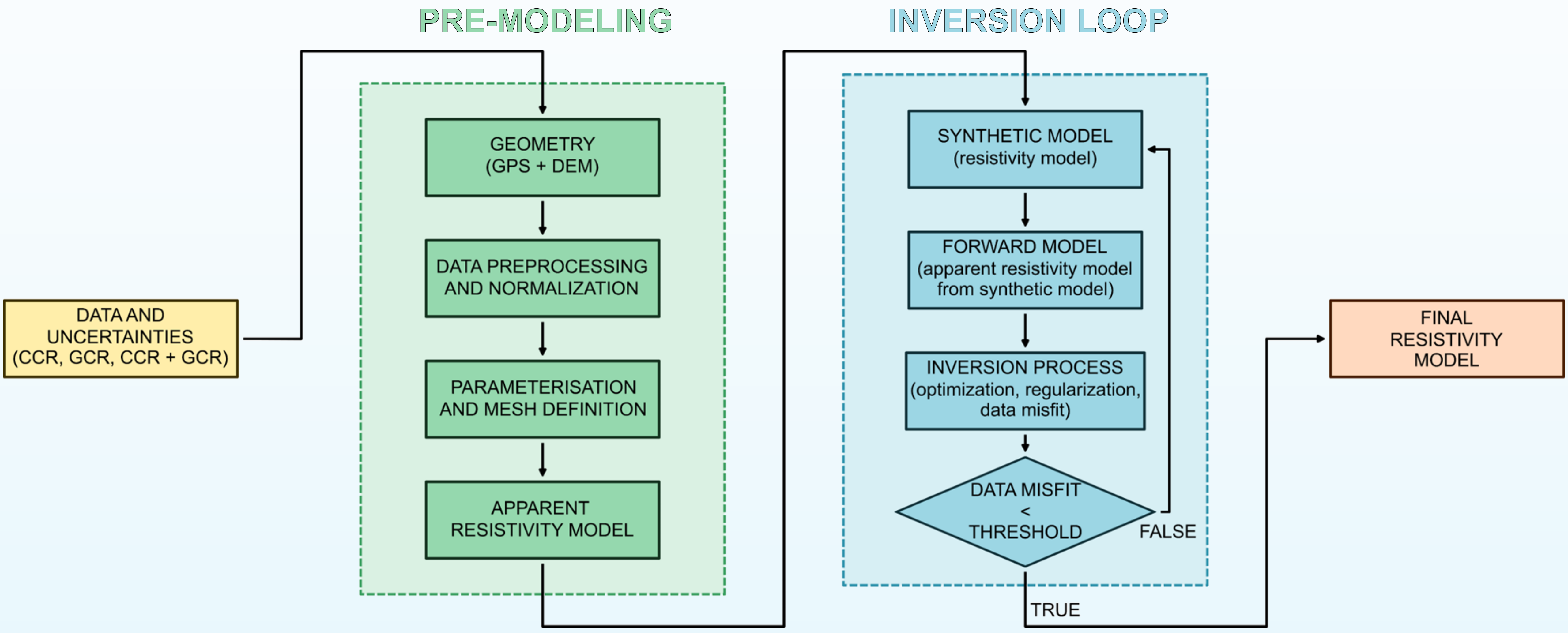

Data inversion processing workflow

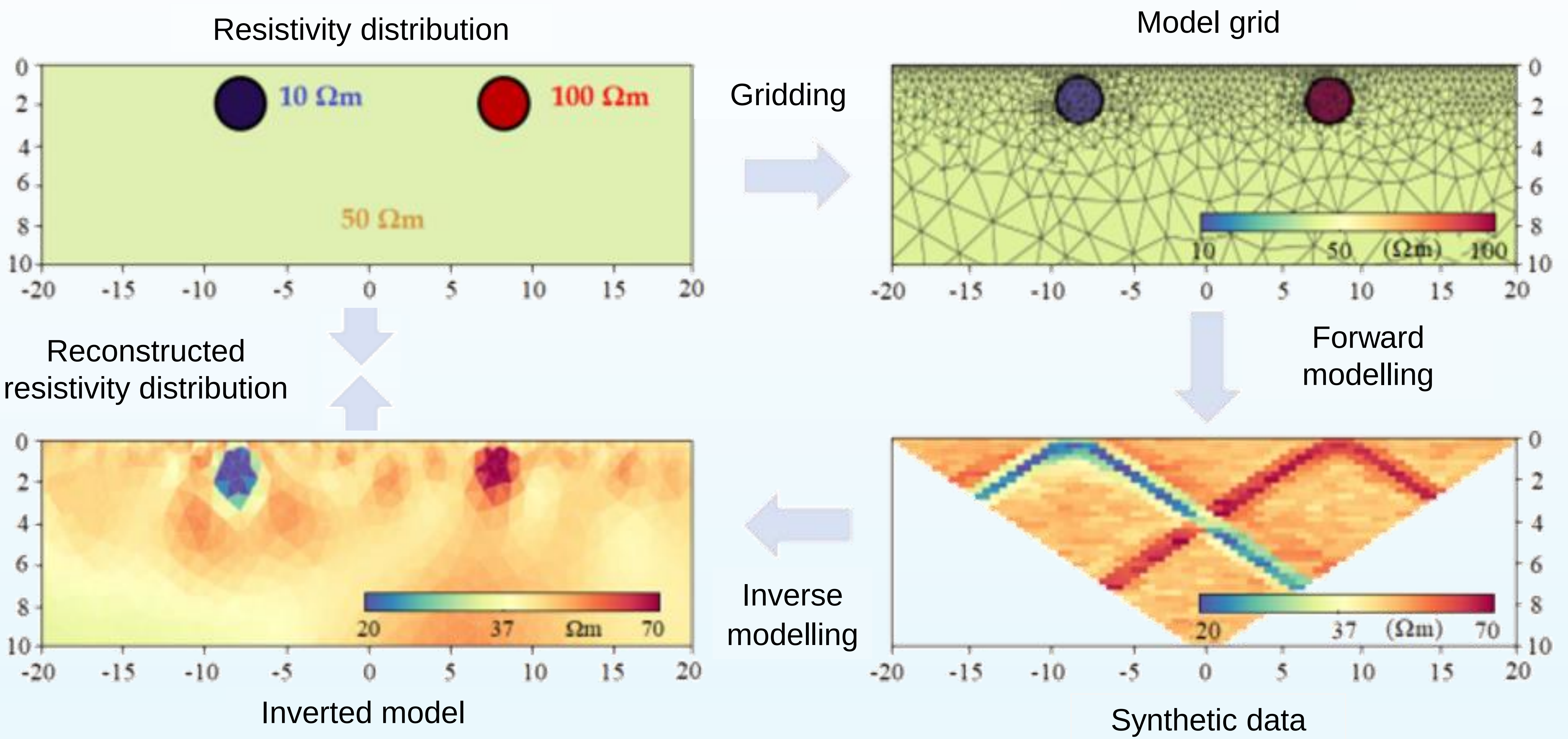

Data processing

Apply correction factor

CCR data inversion is inaccurate due to **systematic bias** affecting the dipole–dipole geometry → A **0.8** correction factor is applied to CCR antenna length to account for non-ideal geometry*

Filter by quality factor

High Q values and **noise** reduce reliability of GCR resistivity measurements → Repeat measurements until **Q < 5% or 5 stacks**; exclude unstable, high-deviation data beyond limit

	GCR	CCR	Joint
N° measurements acquired	5049	384	-
N° input data	4959	384	5343

* M. Neukirch and N. Klitzsch, 'Inverting Capacitive Resistivity (Line Electrode) Measurements with Direct Current Inversion Programs', *Vadose Zone Journal*, vol. 9, no. 4, pp. 882–892, Nov. 2010, doi: 10.2136/vzj2009.0164.

Constraints setting

TreeMesh

- Minimum horizontal cell width (dxy): **0.4 m**
- Minimum vertical cell width (dz): **0.25 m**
- Total mesh extents: **30 m horizontally - 8 m vertically**

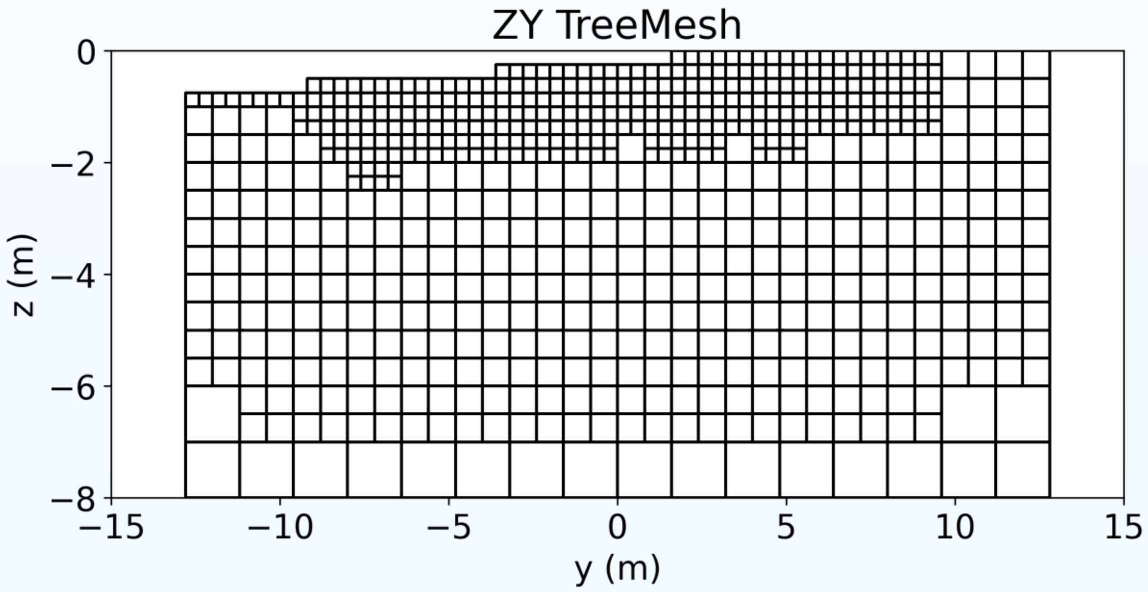

Parametrizations

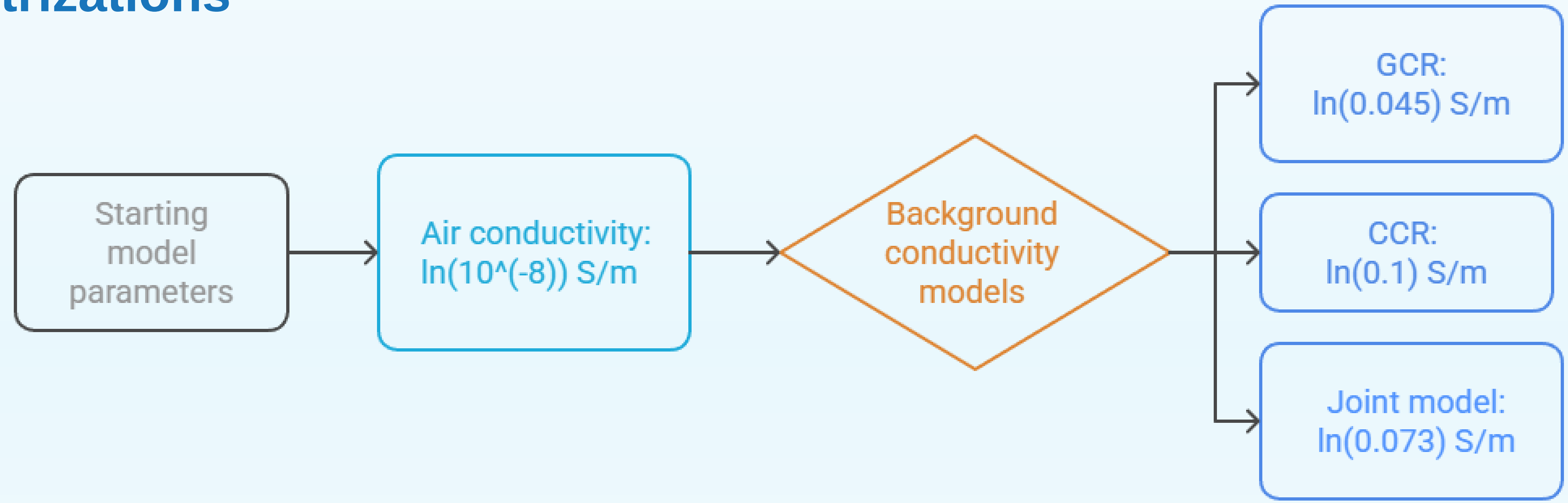

Parameters affecting geoelectrical joint inversion

Inversion objective function

$$\phi(m) = \phi_d(m) + \beta\phi_m(m)$$

$\phi_d(m)$= data misfit

$\beta\phi_m(m)$ = model regularization term

	GCR		CCR		Joint	
	Range	Best	Range	Best	Range	Best
Beta ratio	10^{-4} - 10^{3}	10^{2}	10^{-4} - 10^{3}	10	10^{-4} - 10^{3}	200
ε	10^{-4} - 1	10^{-2}	10^{-4} - 1	10^{-2}	10^{-4} - 1	10^{-2}
Iterations	3 - 50	12	3 - 50	13	3 - 50	14
Tol F	10^{-5} - 10^{4}	0.04	10^{-5} - 10^{4}	0.01	10^{-1} - 10	0.003

β

A value controlling the weight of the regularization in the inversion

Regularization

A term that smooths the model by preventing overly complex solutions

χ^2

Sum of the squared differences between observed and predicted data, normalized by the expected variance

Objective function

Combines data fit and regularization

Studying β - regularization

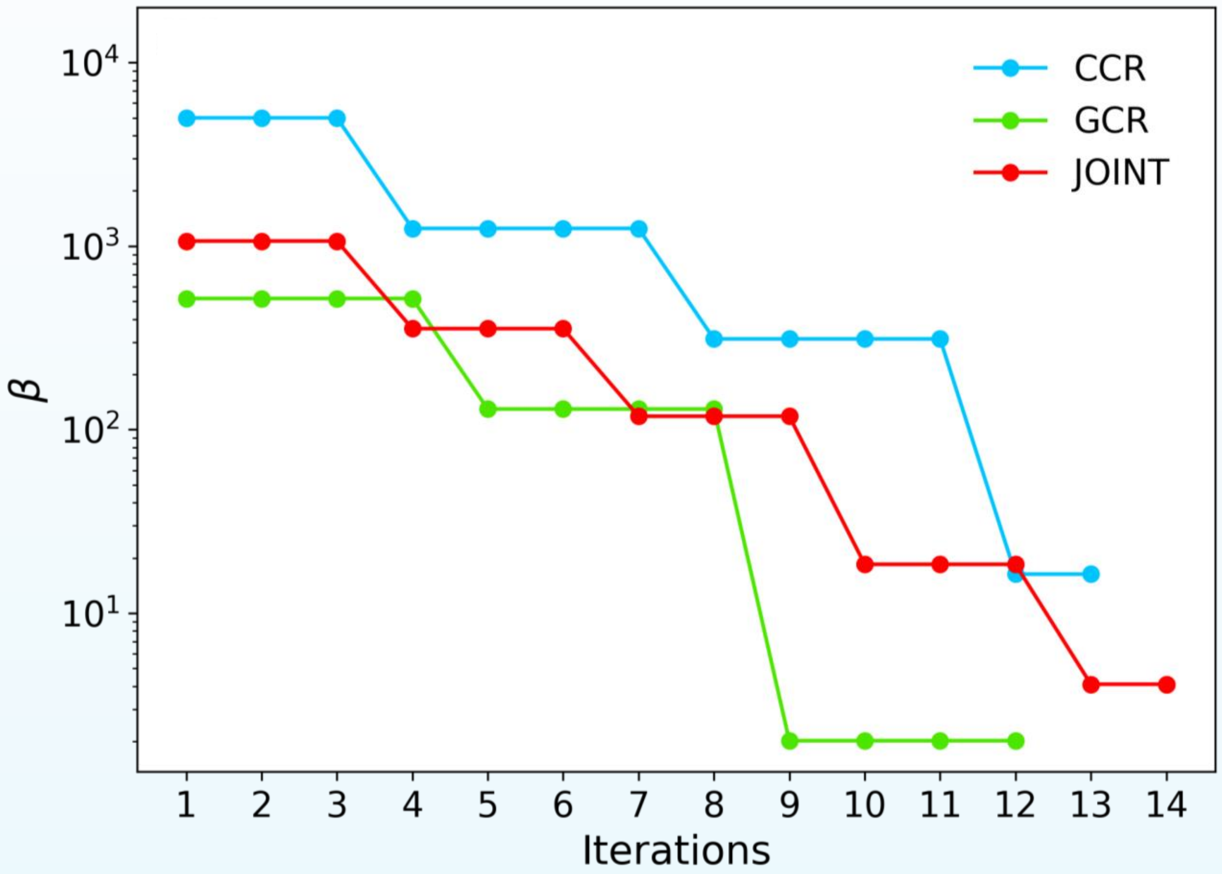

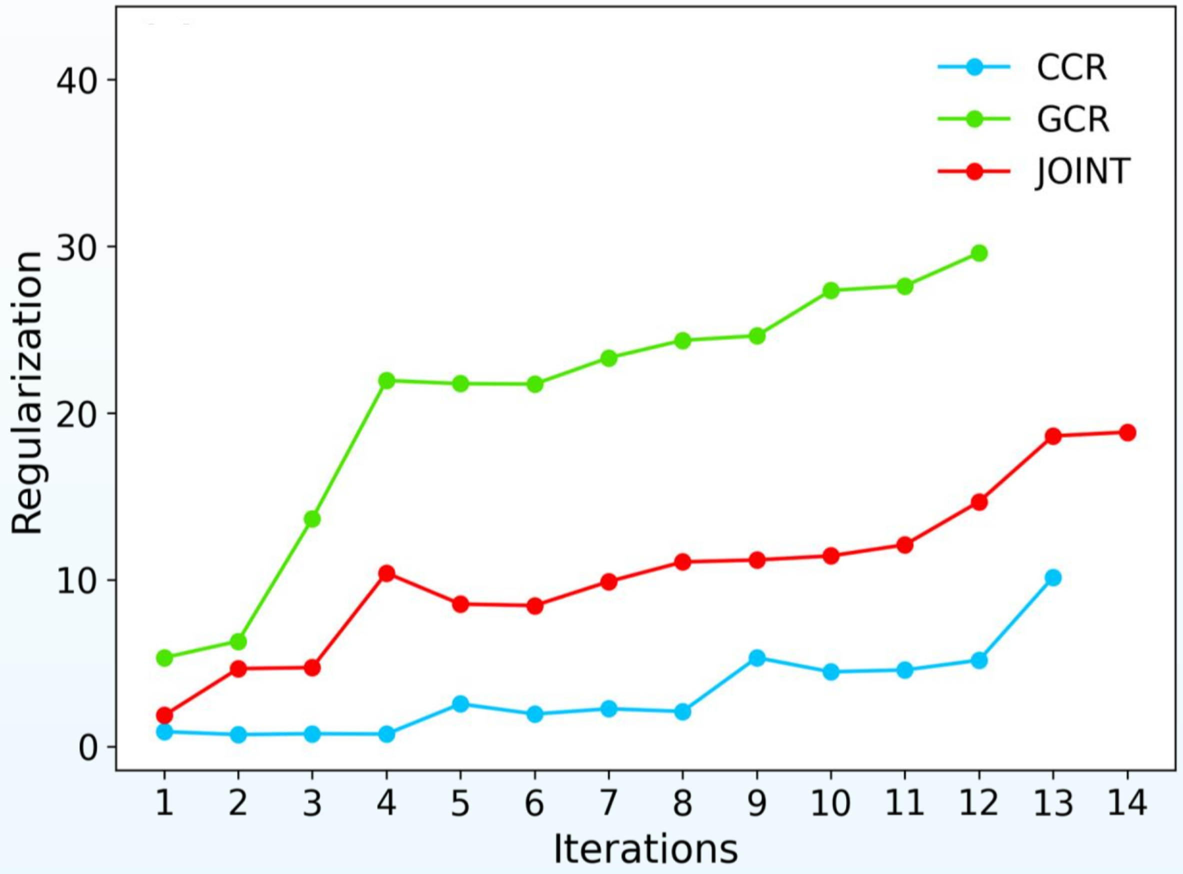

β

Consistent downward trend across all methods, indicating convergence of the inversion and decreasing influence of the regularization term

Regularization

Increases during inversion for all methods, consistent with improved model smoothness adapted to each method’s depth resolution

Studying objective function

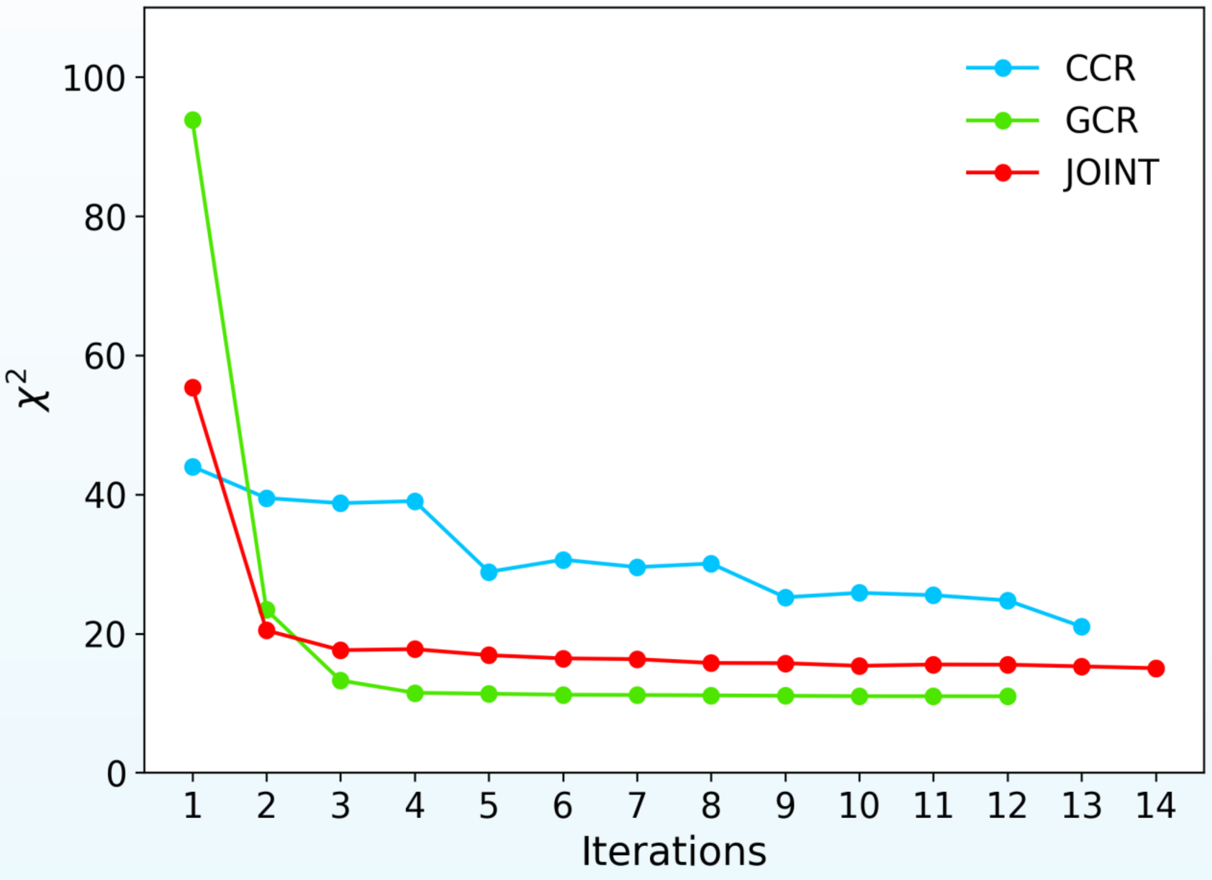

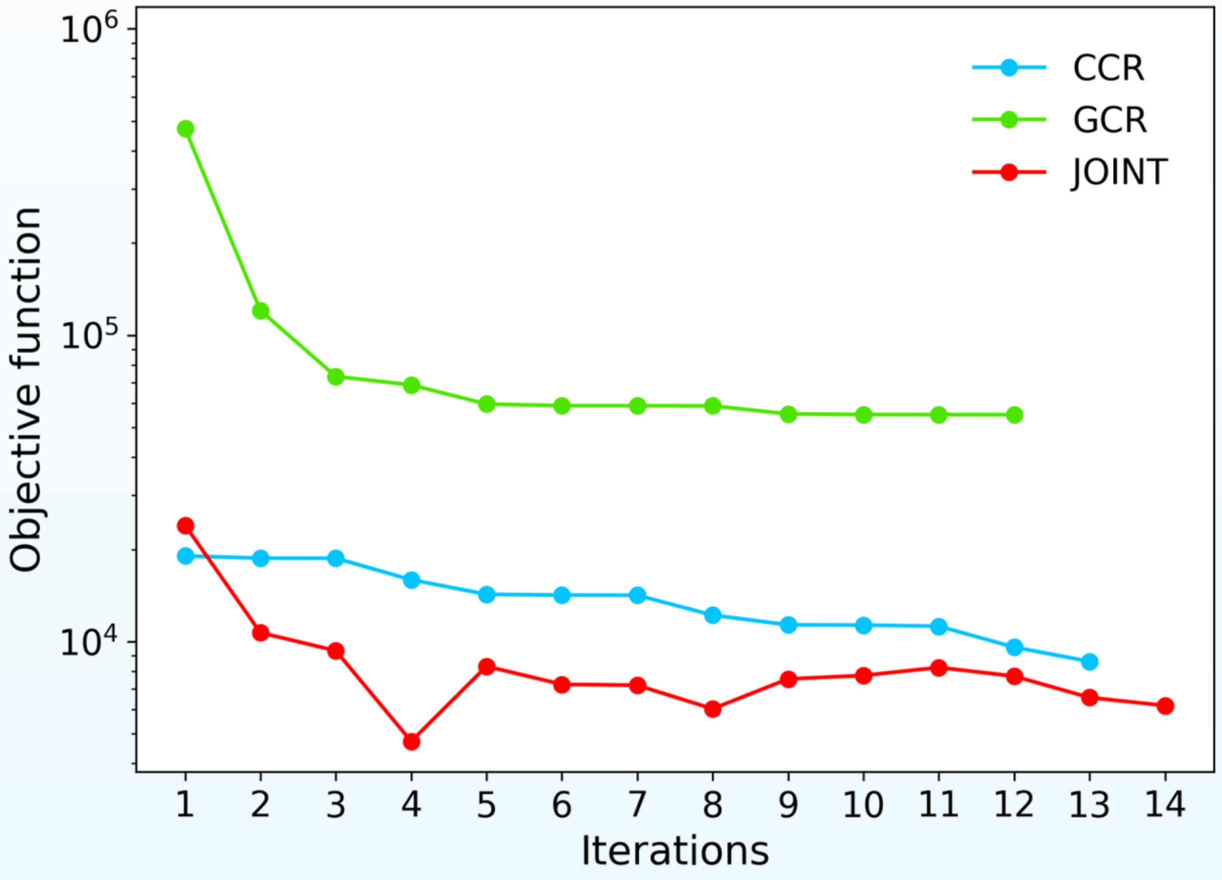

χ^2

Decreases from CCR to GCR, with the joint inversion showing intermediate values, reflecting differences in sensitivity to depth and resistivity contrasts

Objective function

Reaches its lowest level in the joint inversion, confirming its effectiveness in balancing data fit and model regularity

Resistivity sections: GCR vs CCR

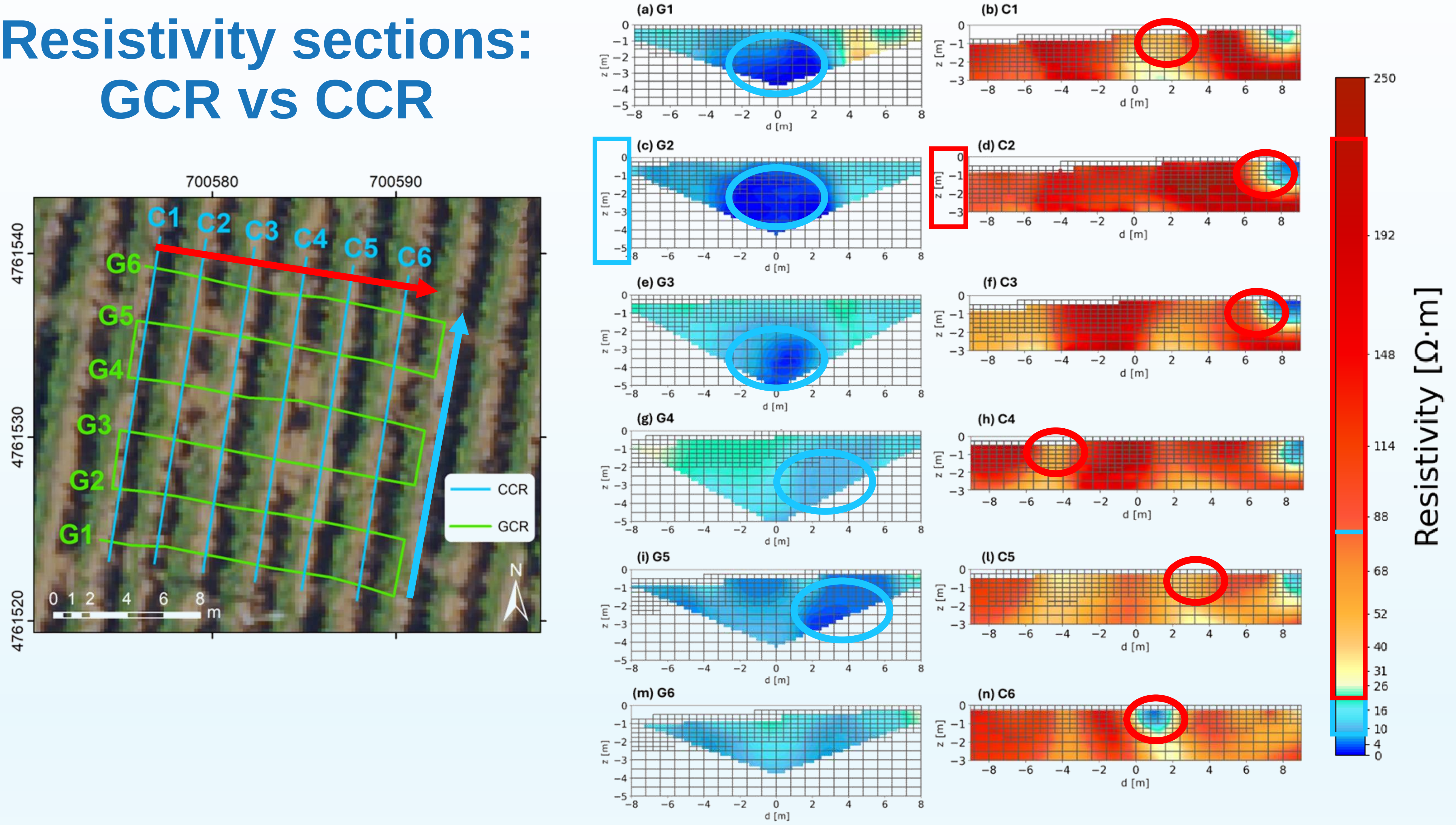

Joint resistivity sections

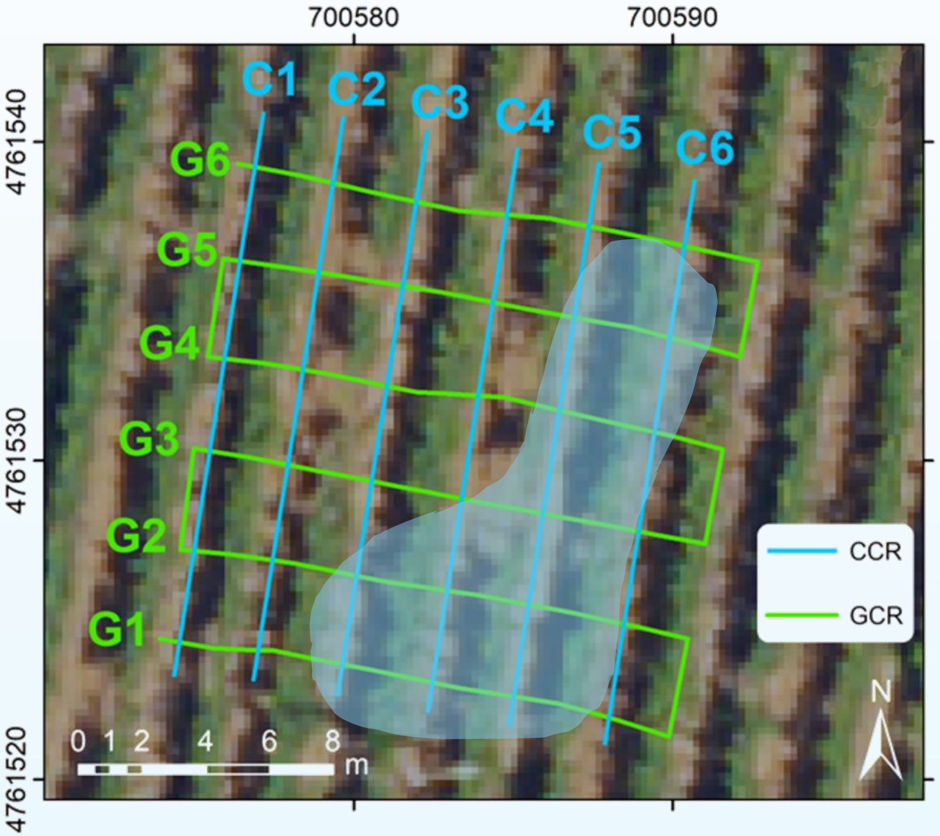

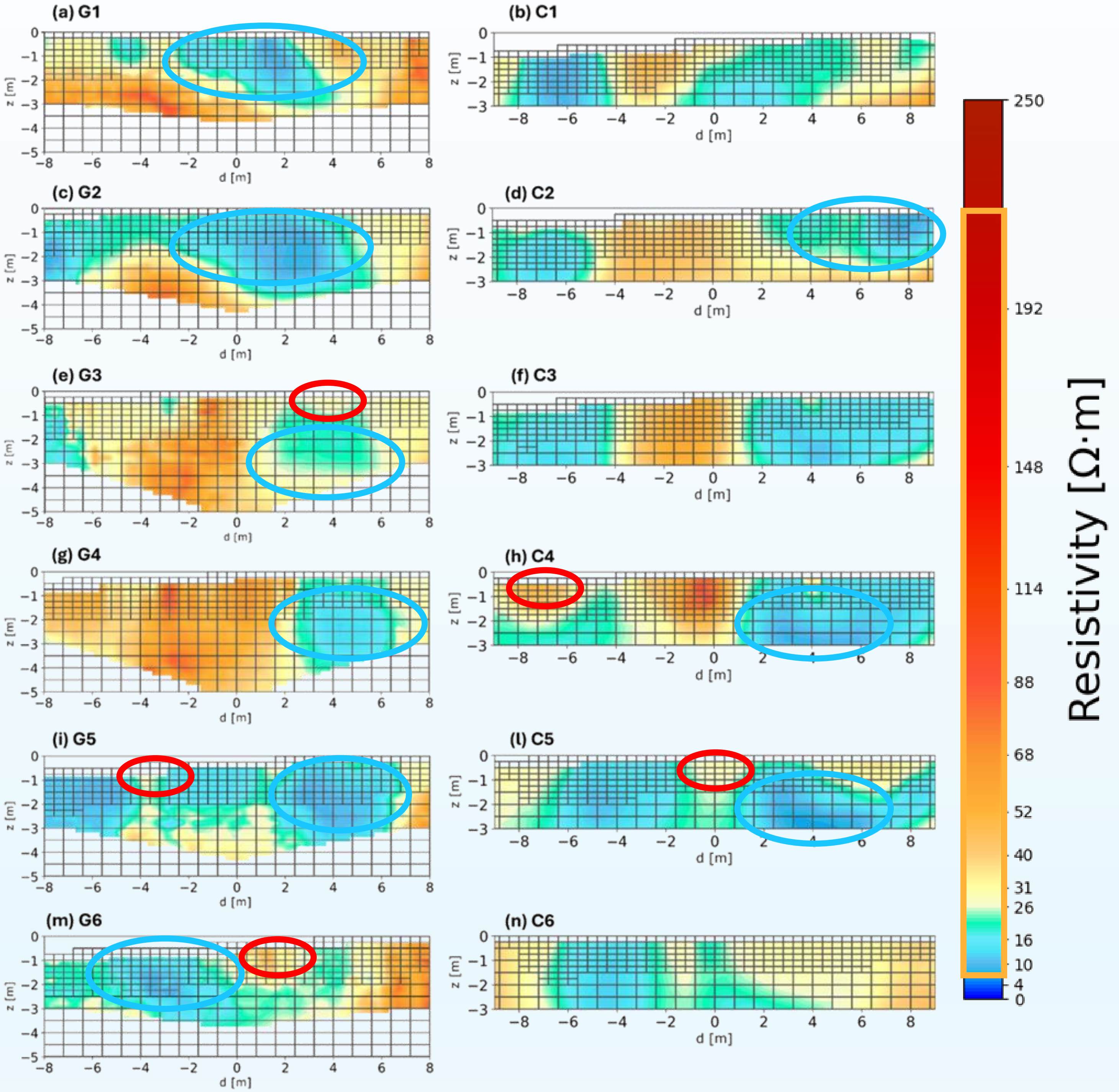

GCR-CCR vs Joint results

GCR (up to 5 meters depth)

- Probes deeper layers
- Good depth coverage but loses spatial resolution

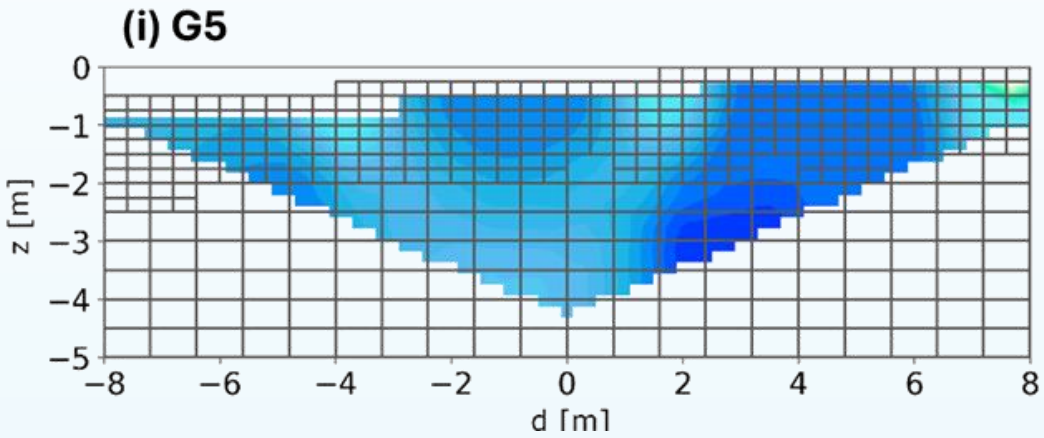

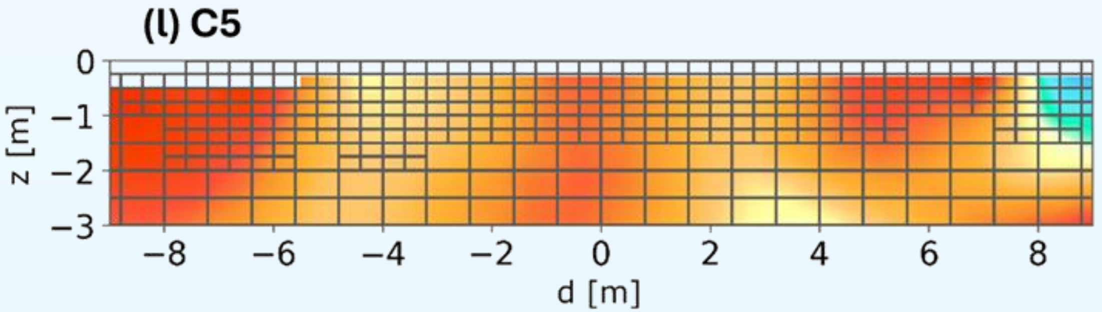

CCR (up to 3 meters depth)

- High-resolution data for shallow layers
- Reduced accuracy at greater depths

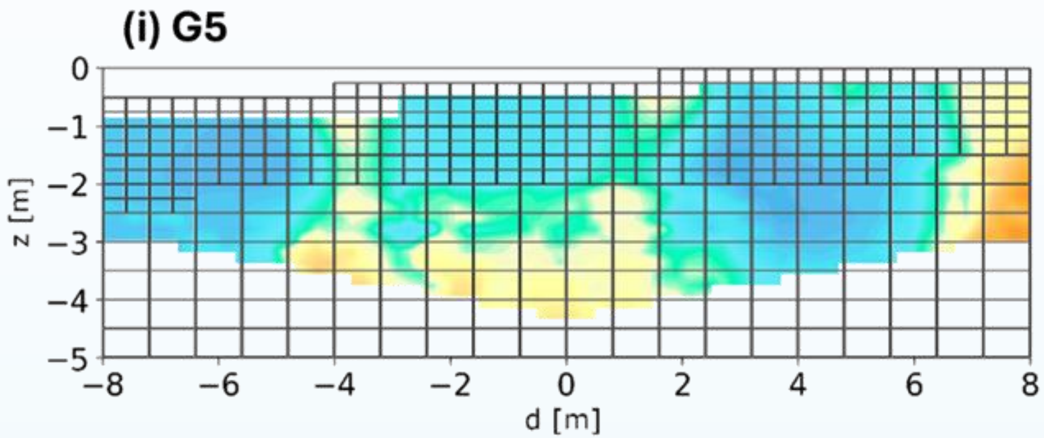

Joint Inversion

- Combines strengths of both methods
- Comprehensive 3D model integrating shallow resolution from CCR and deeper probing from GCR

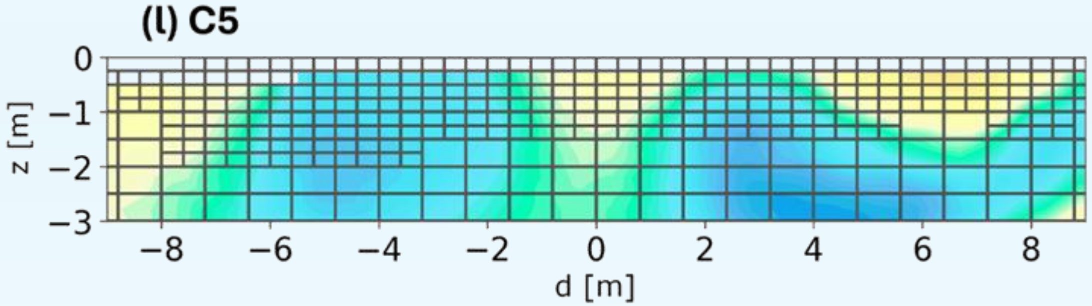

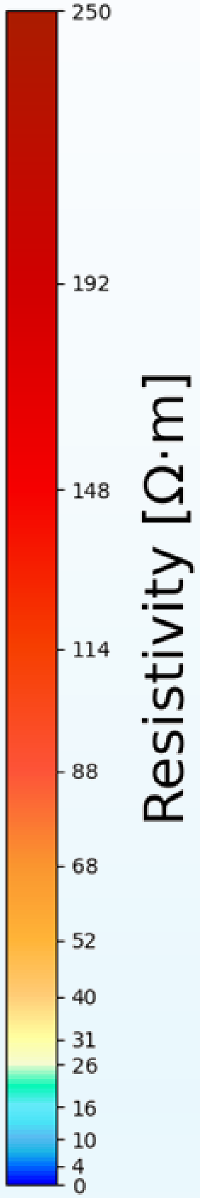

Model performance and misfit analysis

$$\phi_{d-joint}(m) = (1-\alpha)\phi_{d-GCR}(m) + \alpha\,\phi_{d-CCR}(m)$$

α= weighted ratio (0-1) $\phi_d(m)$= data misfit

$$Misfit = \frac{\sqrt{\sum_{i=1}^{N}\left(D_{obs,i} - D_{syn,i}\right)^2}}{n}$$

Single-objective models

Each model simulates one acquisition setup. Synthetic data align with its own observations but misfit increases when evaluated against non-corresponding acquisition data

		Model		
Data		GCR	CCR	Joint
	GCR	$1.04 \cdot 10^{-2}$	$27.5 \cdot 10^{-2}$	$2.80 \cdot 10^{-2}$
	CCR	$2.10 \cdot 10^{-2}$	$1.91 \cdot 10^{-2}$	$1.95 \cdot 10^{-2}$

Joint inversion

A single model integrates both acquisition setups. Synthetic data capture varying sensitivities, allowing coherent fit across datasets and improved assessment of shared model regions

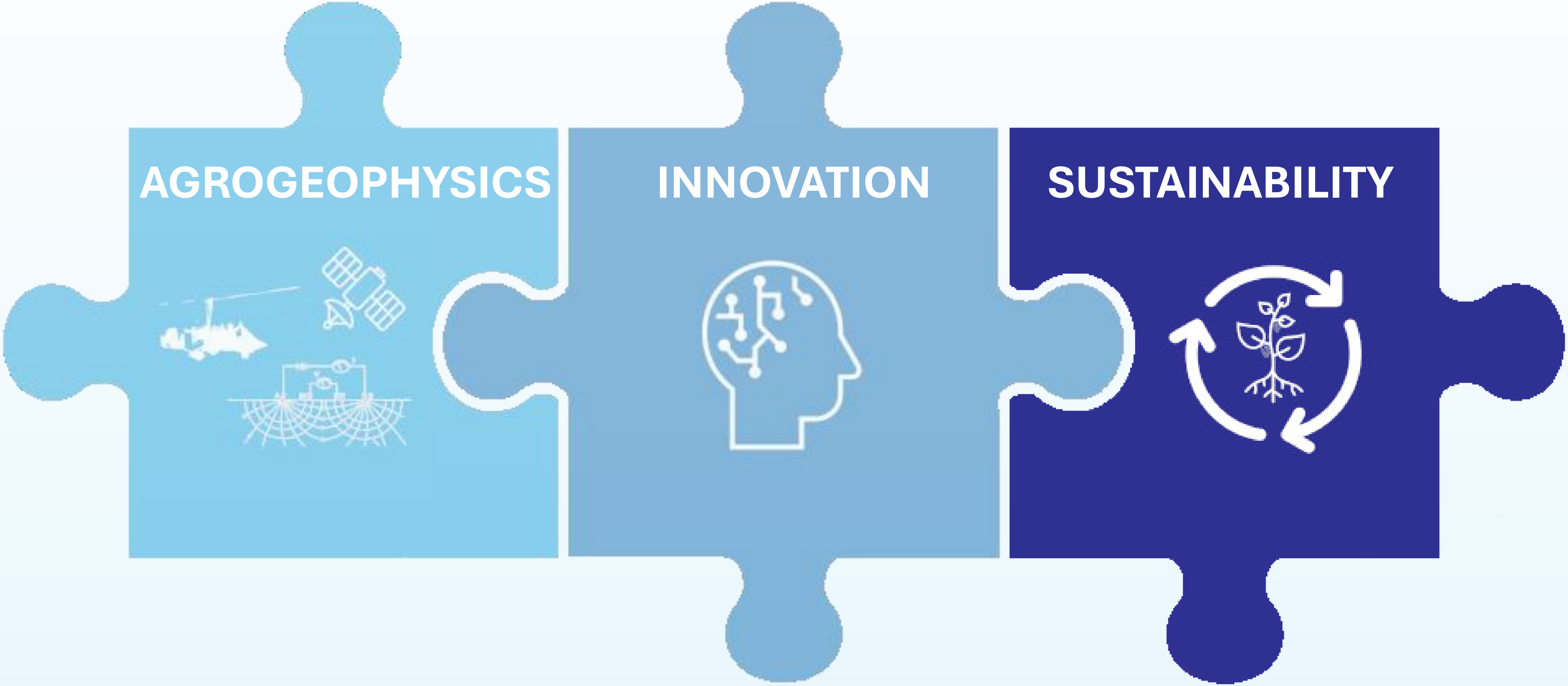
AGROGEOPHYSICS
INNOVATION
SUSTAINABILITY

Vineyard root mapping via joint inversion

- Joint inversion detects roots via resistivity contrasts from **moisture** and **electrolyte** changes by root activity
- **Thicker roots** show higher resistivity; **thinner roots** lower resistivity, revealing structure and distribution
- Root morphology and function comprehensively characterized to **1 m depth** through resistivity patterns

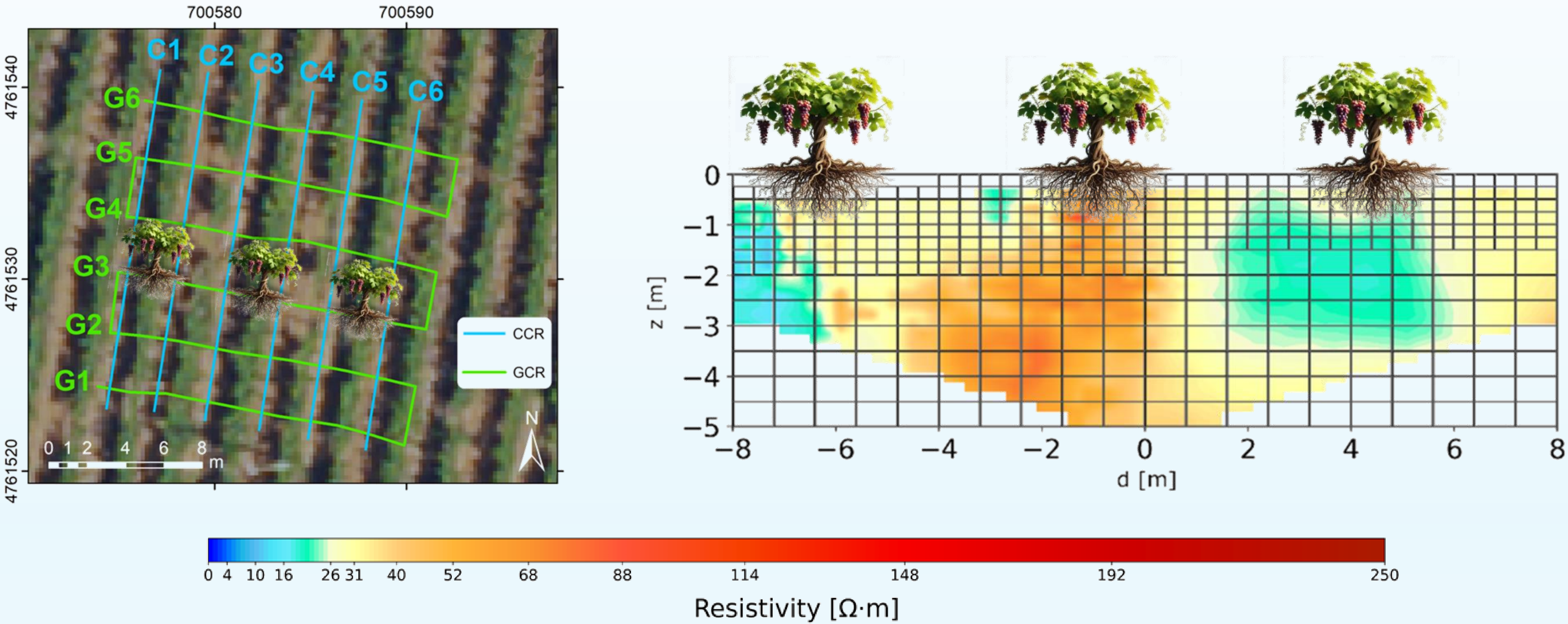

Insights from 3D resistivity model

Zones of low resistivity (<20 Ω·m)
subsurface water

Agronomic implications

Water distribution
Impact on vine health:
excess water = trunk diseases

Vineyard management strategies

Targeted interventions:
farming practices - soil variability

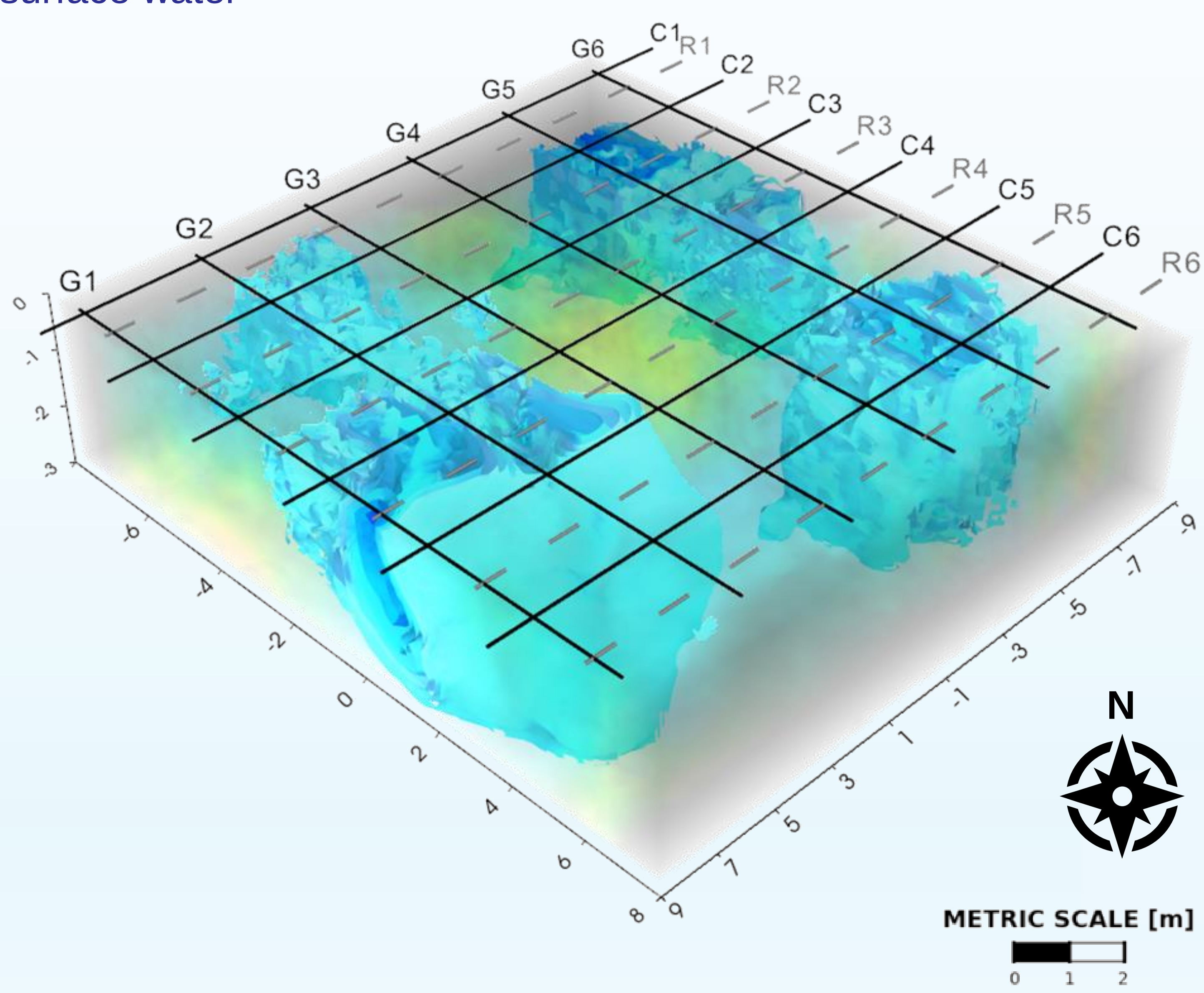

Joint resistivity profiles

Unplowed soil

Higher resistivity due to better water infiltration into deeper layers

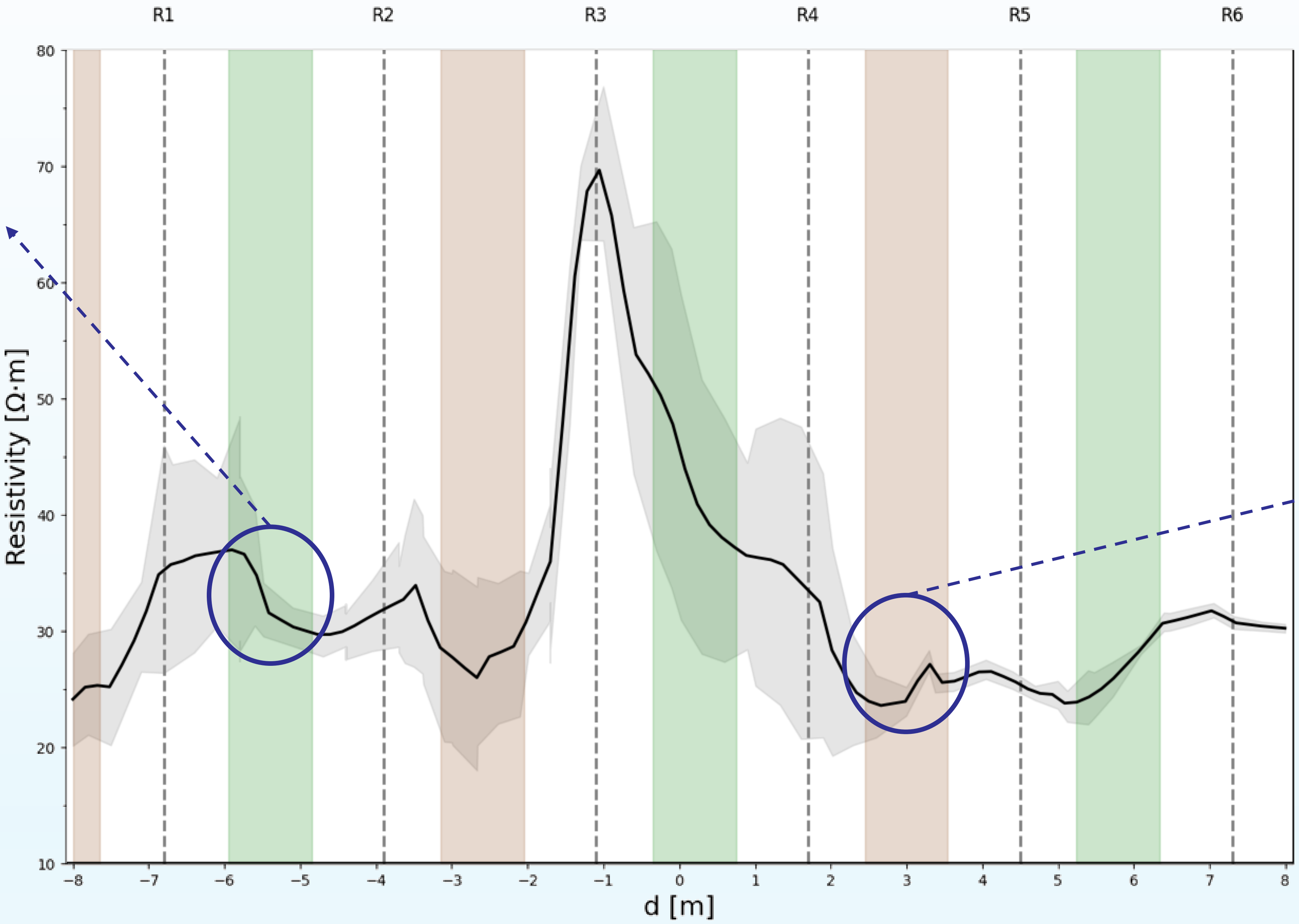

Plowed soil

Lower resistivity from compaction and reduced porosity, limiting deep water infiltration

Eco-driven solutions

OBJECTIVE

- Develop a 3D resistivity model with a high spatial resolution of 20.21 data/m³ using CCR and GCR data
- Improve subsurface soil characterization

BENEFIT

- Reduces data misfit more effectively than individual inversions
- Provides a smooth integration of shallow and deep subsurface data

SIGNIFICANCE

- Identifies key features like subsurface water and the effects of soil management
- Provides tools to optimize wine quality and vine health

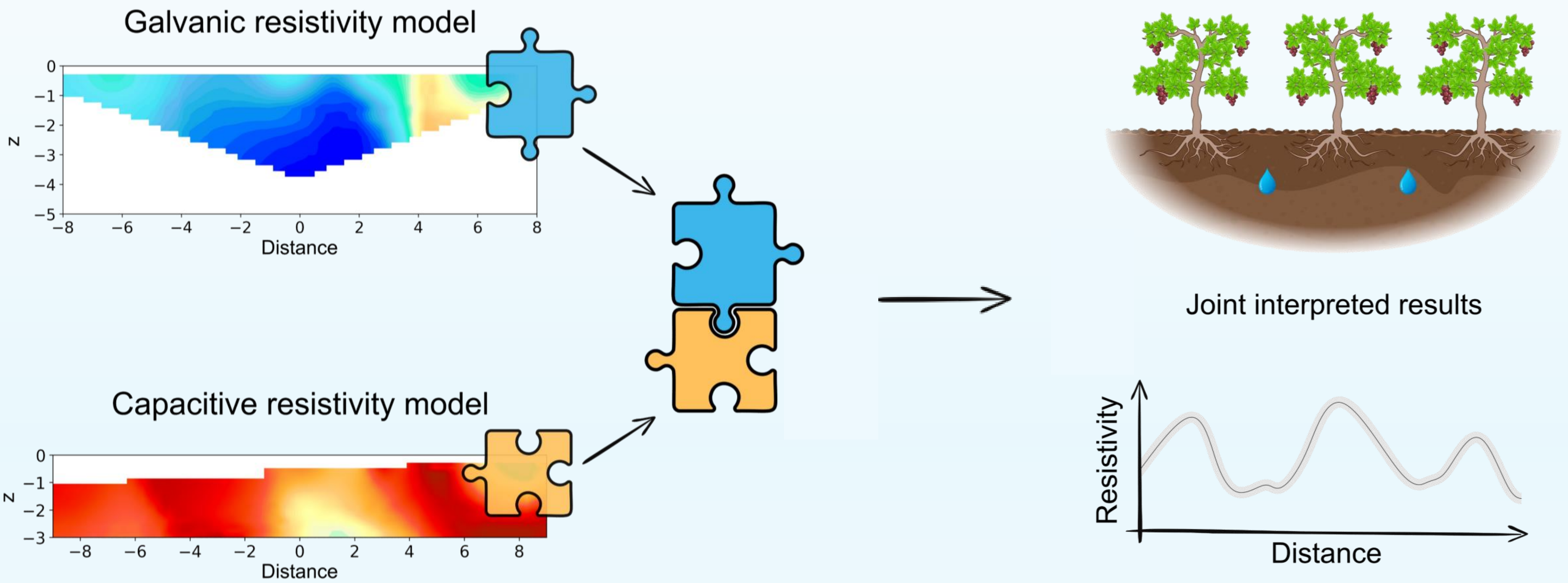

Future directions

Real-time monitoring

Adaptive management of soil and water resources.

Precision integration

Accurate resource allocation using joint inversion techniques.

3D Imaging & remote sensing

High-resolution analysis from root zones to landscapes.

What I really understood from my PhD?

Interdisciplinarity

New knowledge emerged through engineered collisions of fields

Sustainability

A once-elusive ideal reframed through empirical grounding

Innovation

Technical refinement translated complexity into clarity

Practical tools

"Is this useful to the people who need it?"

Collaboration

Complexity demanded alliances over isolated expertise

From vines to landscapes

Research applications extending beyond initial focus


THANK YOU FOR YOUR ATTENTION!

Agrogeophysical methods and tools

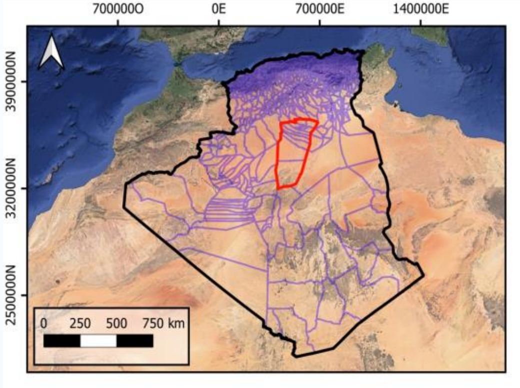

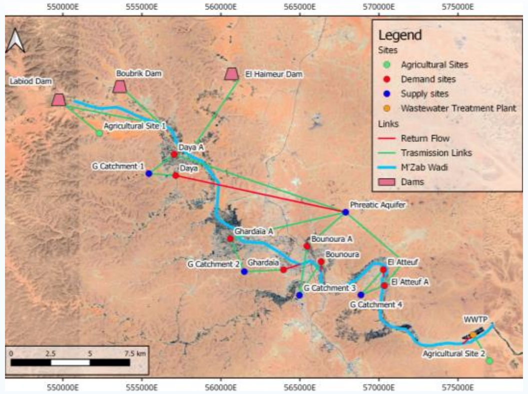

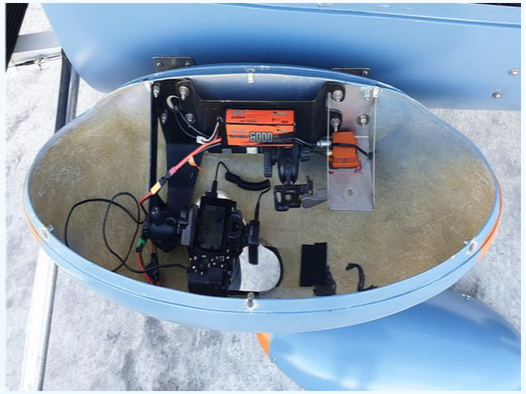

SATELLITE REMOTE SENSING

$$\mathrm{NDVI} = \frac{NIR - RED}{NIR + RED} \qquad \Delta S = P - ET - R - Q$$

- Tracks agricultural expansion and urbanization
- Geophysical analysis of spatial land dynamics

AIRBORNE SENSORS

$$\mathrm{GRVI} = \frac{\rho_G - \rho_R}{\rho_G + \rho_R} \qquad \mathrm{GBVI} = \frac{\rho_G - \rho_B}{\rho_G + \rho_B} \qquad \mathrm{BRVI} = \frac{\rho_B - \rho_R}{\rho_B + \rho_R}$$

- Reflectance (ρ) maps chlorophyll in RGB bands
- High efficiency and good spectral resolution

GEOELECTRICAL METHODS

$$V = IR \qquad \rho_a = k\,\frac{V}{I}$$

- Maps soil resistivity (Ω·m) in 3D
- Reveals moisture, texture, and structure
- Detects salinity and compaction

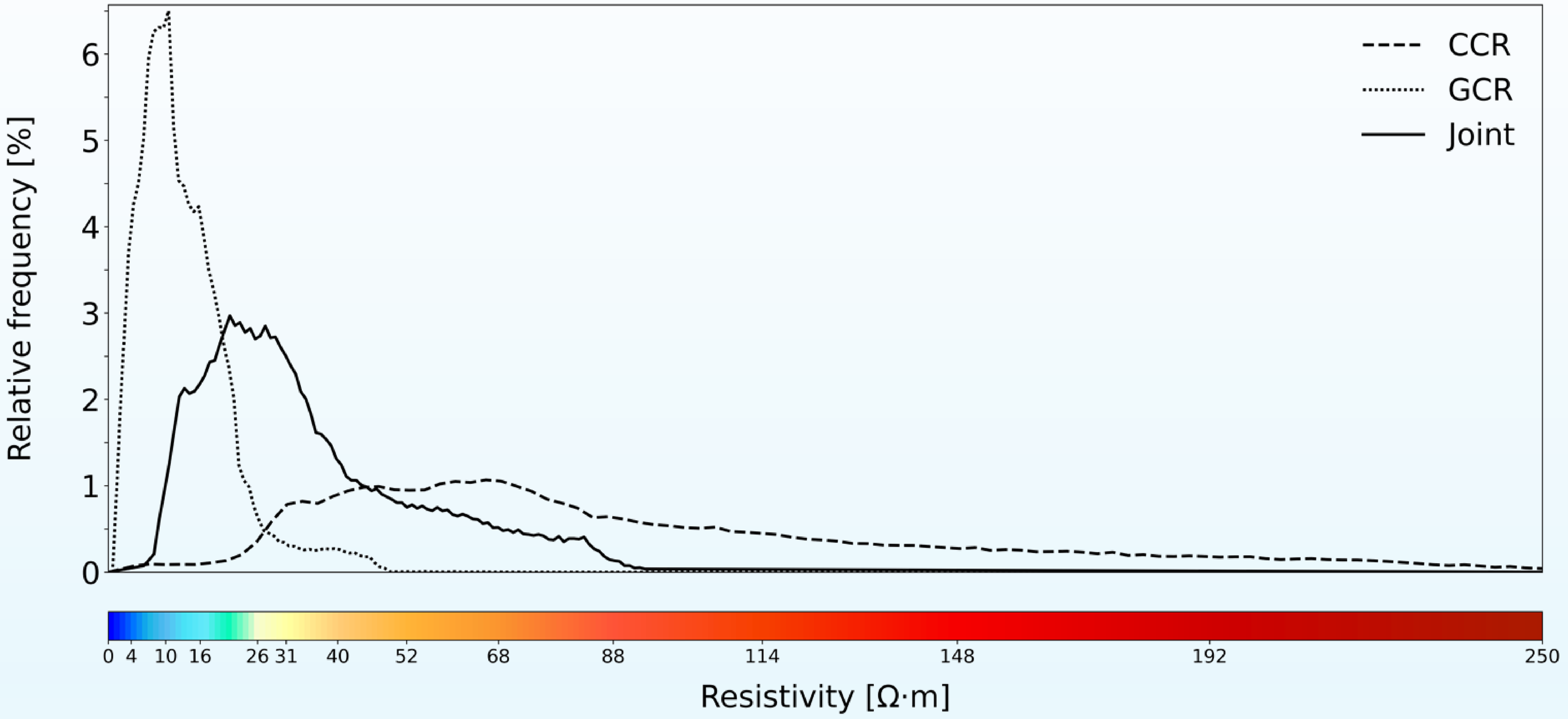

CCR
GCR
Joint
Relative frequency [%]
0
1
2
3
4
5
6
0 4 10 16 26 31 40 52 68 88 114 148 192 250
Resistivity [Ω·m]

What is agrogeophysics?

Agrogeophysics uses geophysical methods to study soil and water dynamics for agricultural optimization

- **How do we analyze soil properties?**

- **How do soil-plant-atmosphere interactions affect water and nutrient dynamics?**

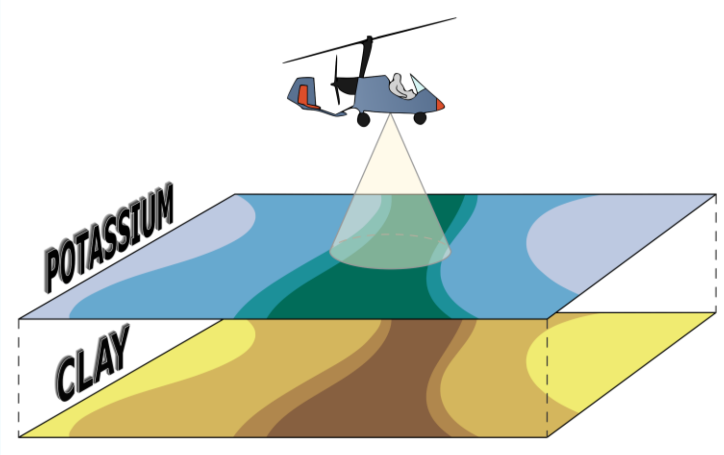

- **How can geophysical data optimize resource management?**

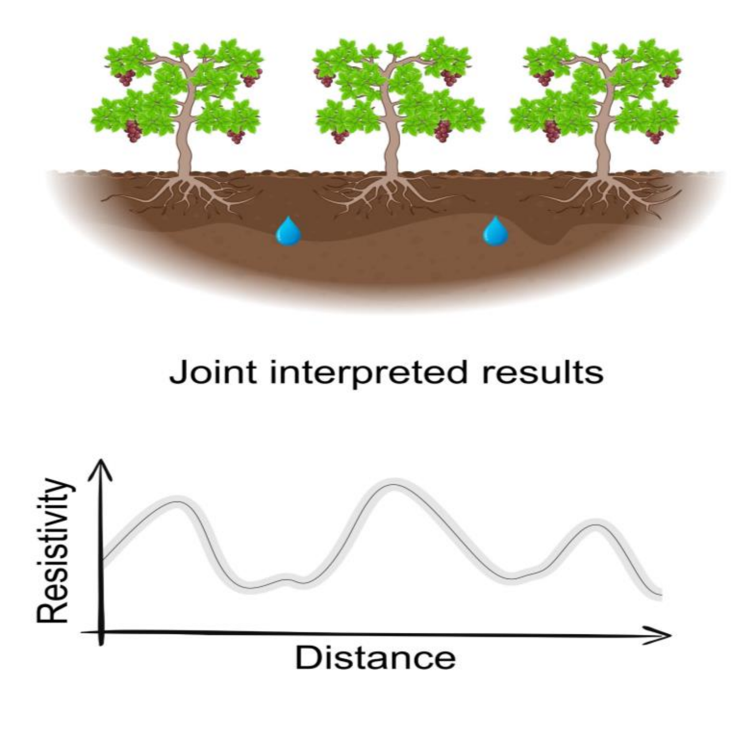

Airborne methods in agriculture

- **Soil texture mapping** is essential for precision agriculture and targeted interventions.
- For large areas, **direct measurement** methods are **wasteful** in terms of time and money.
- **Airborne Gamma Ray Spectroscopy (AGRS)** overcomes these issues allowing for a fast and efficient mapping of large areas.

- **Flavescence Dorée** severely damages vineyards, demanding early detection
- **Ground inspections** are slow and fail to detect early symptoms
- **High-resolution airborn imaging** detects infected plants early and generates actionable maps.

Experimental sites via airborne analysis

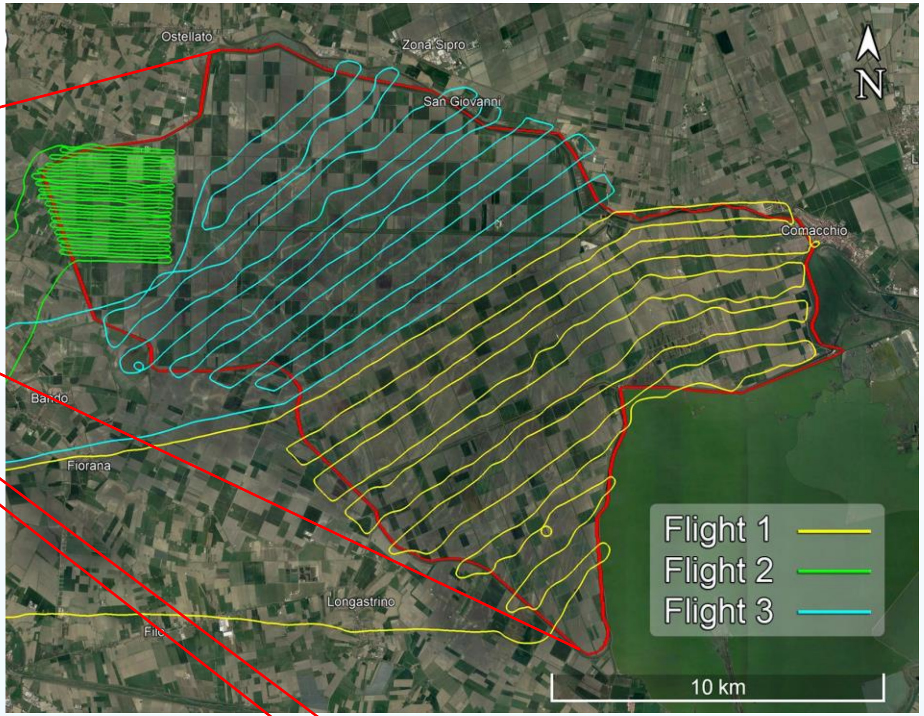

Mezzano lowland, Ferrara

- 3 surveys: (~ **189 km^2**) **4 hours and 45 minutes**.
  - Mean **flight height** of 104 ± 21 m
  - Mean **velocity** of 102 ± 13 km/h
  - Field of view (FOV) of **radius 300 m**
  - Measurements every **300 m**.
- Gamma spectra acquired with a time resolution of 10 s for a total of **1469 spectra**.

Forlì

- (**17.1 hectares vineyard**) **~5600 plants/ha**
  - Mean **flight height** of 96 m
  - Mean **velocity** of 73 km/h
  - Line spacing **25 m.**
- 1015 georeferenced photograms

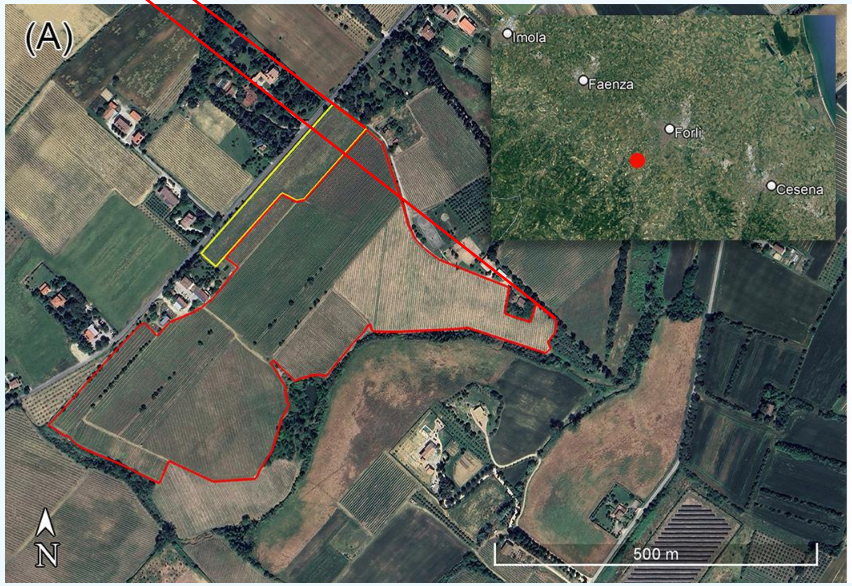

Instrumentation and analysis

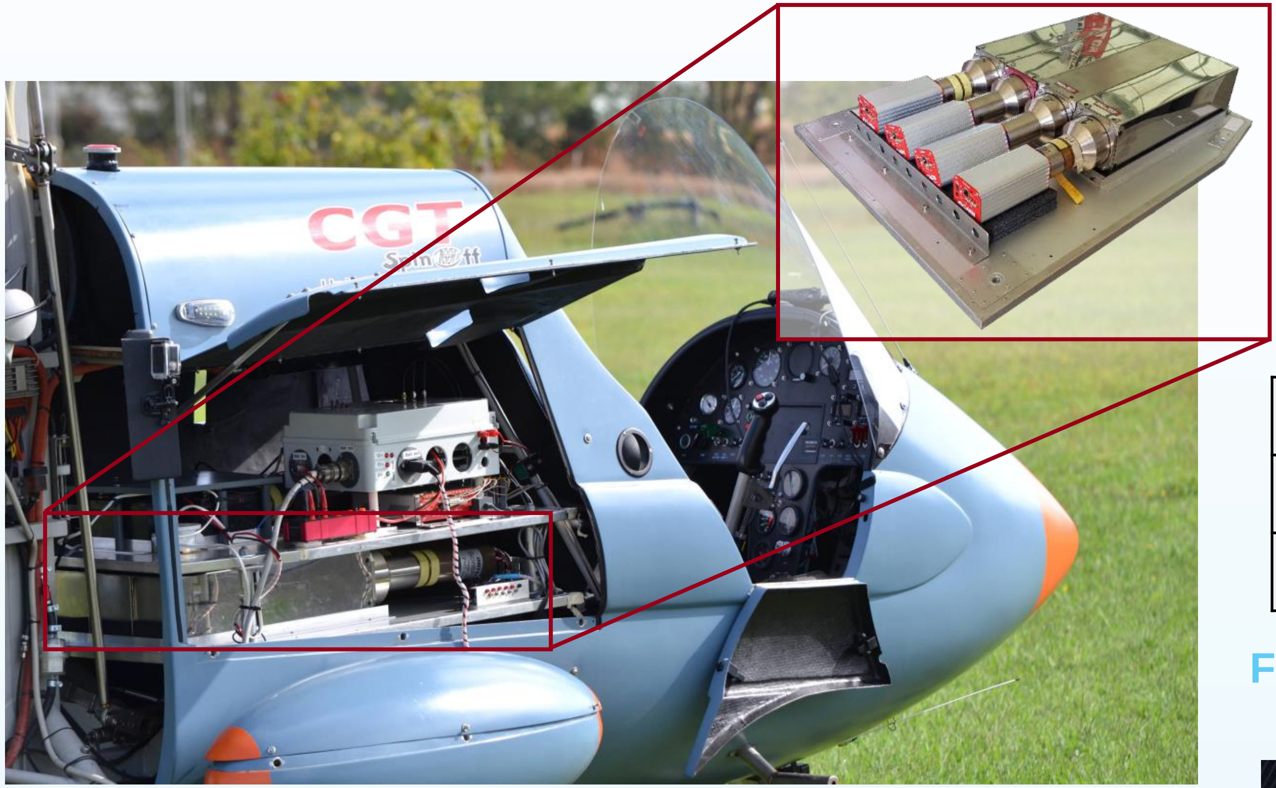

16 L NaI(Tl) crystals surrounded by 1 mm thick stainless steel housings (4 modules).

6.8 % energy resolution at 662 keV (^{137}Cs).

Minimum Detectable activity **Concentration (MDC)** and **Abundance (MDA)**:

	MDC	MDA	
^{40}K	16 Bq/kg	$0.05 \cdot 10^{-2}$ g/g	K
^{238}U	4.94 Bq/kg	0.4 µg/g	U
^{232}Th	3.25 Bq/kg	0.8 µg/g	Th

Full spectrum analysis with ^{137}Cs, ^{40}K, ^{238}U and ^{232}Th simulated fundamental spectra (assuming secular equilibrium conditions)

Camera: Sony α 7R IV Mirrorless Full-Frame, 61 MP, 35 mm lens, nadiral position for high-quality frames

Image quality: 1.1 cm/pixel resolution with >65% overlap (consecutive) and >70% overlap (adjacent)

1.1 cm x 1.1 cm **orthomosaic**

Unpacking the Machine Learning algorithm

- Data flows sequentially **from left to right** in the architecture
- Each node in **layer *i*** connects to all nodes in the previous **layer *j*.**
- Node: input multipied by a weight → summing the results → adding a bias → applying an activation function

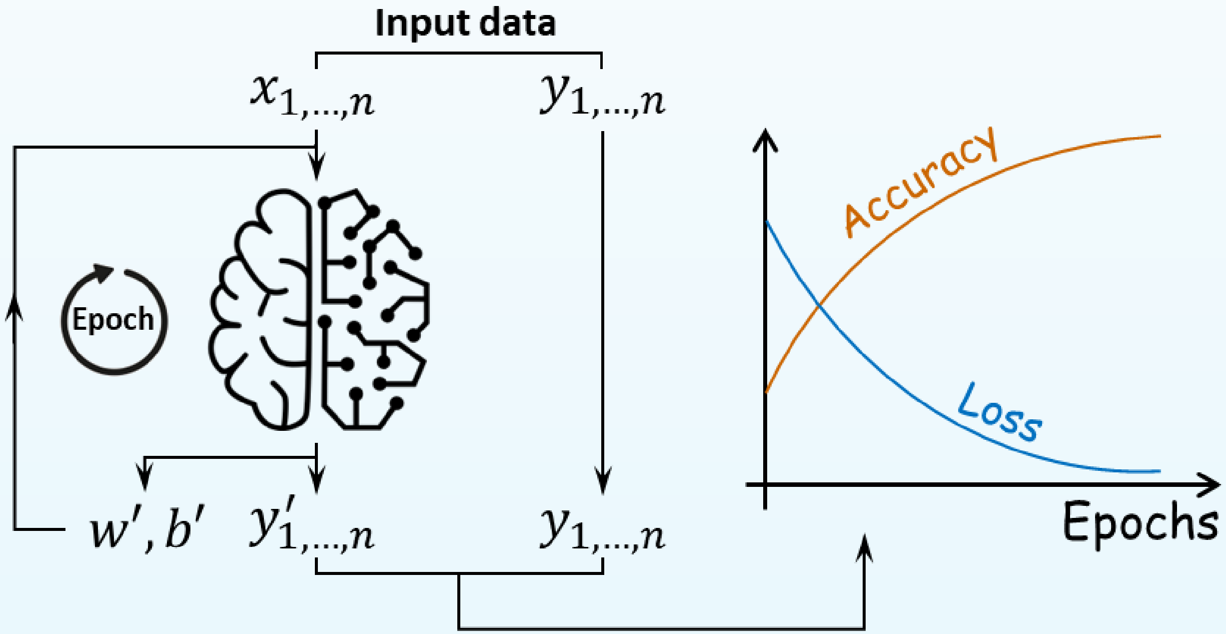

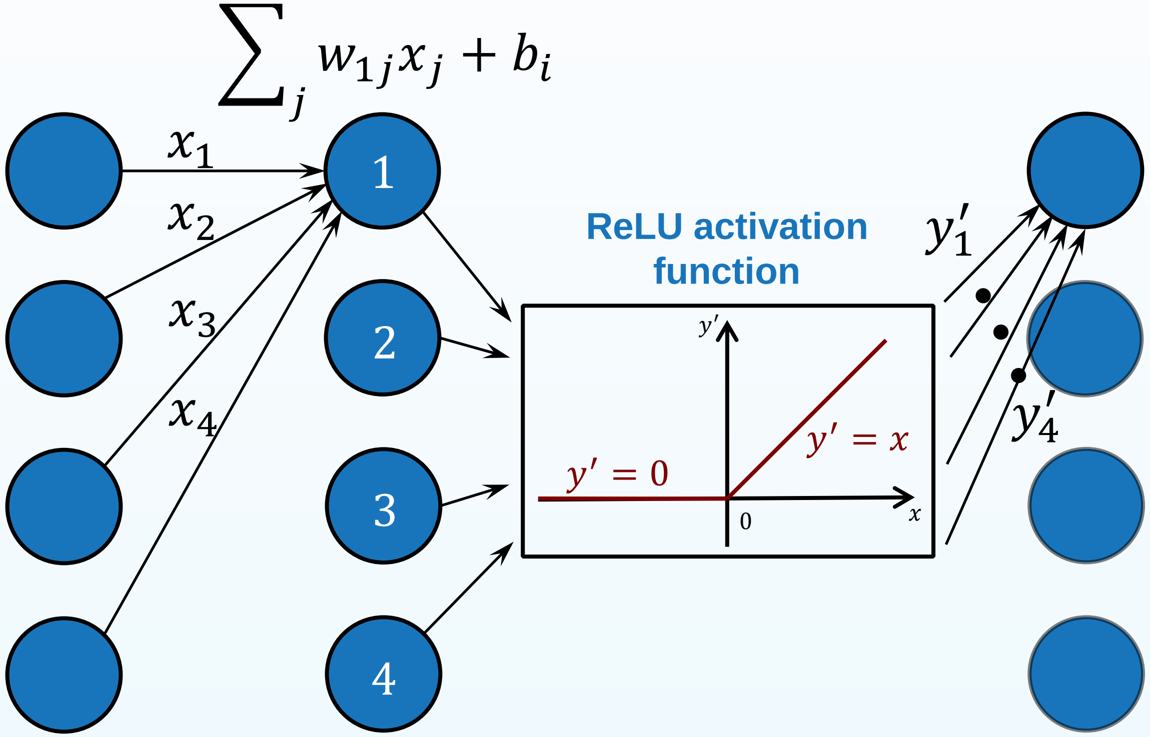

$$y'_i = f\left(\sum_j w_{ij} x_j + b_i\right)$$

The algorithm processes processes data over **epochs**
Weights and biases updated after each epoch
Performance evaluated via **accuracy and loss**

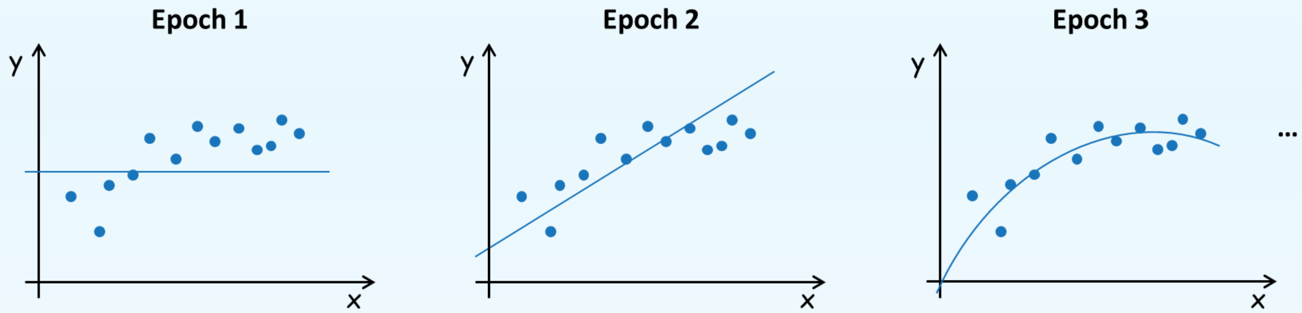

Hyperparameters tuning

Hyperparameters chosen by **trial and error**

Hyperparameters	Tested values
Layer number	2 - **4** - 8
Layer density	4 - **16**
Optimizer	Adadelta, Adagrad, **Adam**, Adamw, Adamax, Nadam, Adafactor, Ftrl, RMSprop and SGD
Batch size	4 – 8 – **16** – 32 - 64
Epoch number	max 40
Learning rate	10^{-4} - $\mathbf{10^{-3}}$ - 10^{-2} - 10^{-1}
Activation function	**ReLU**

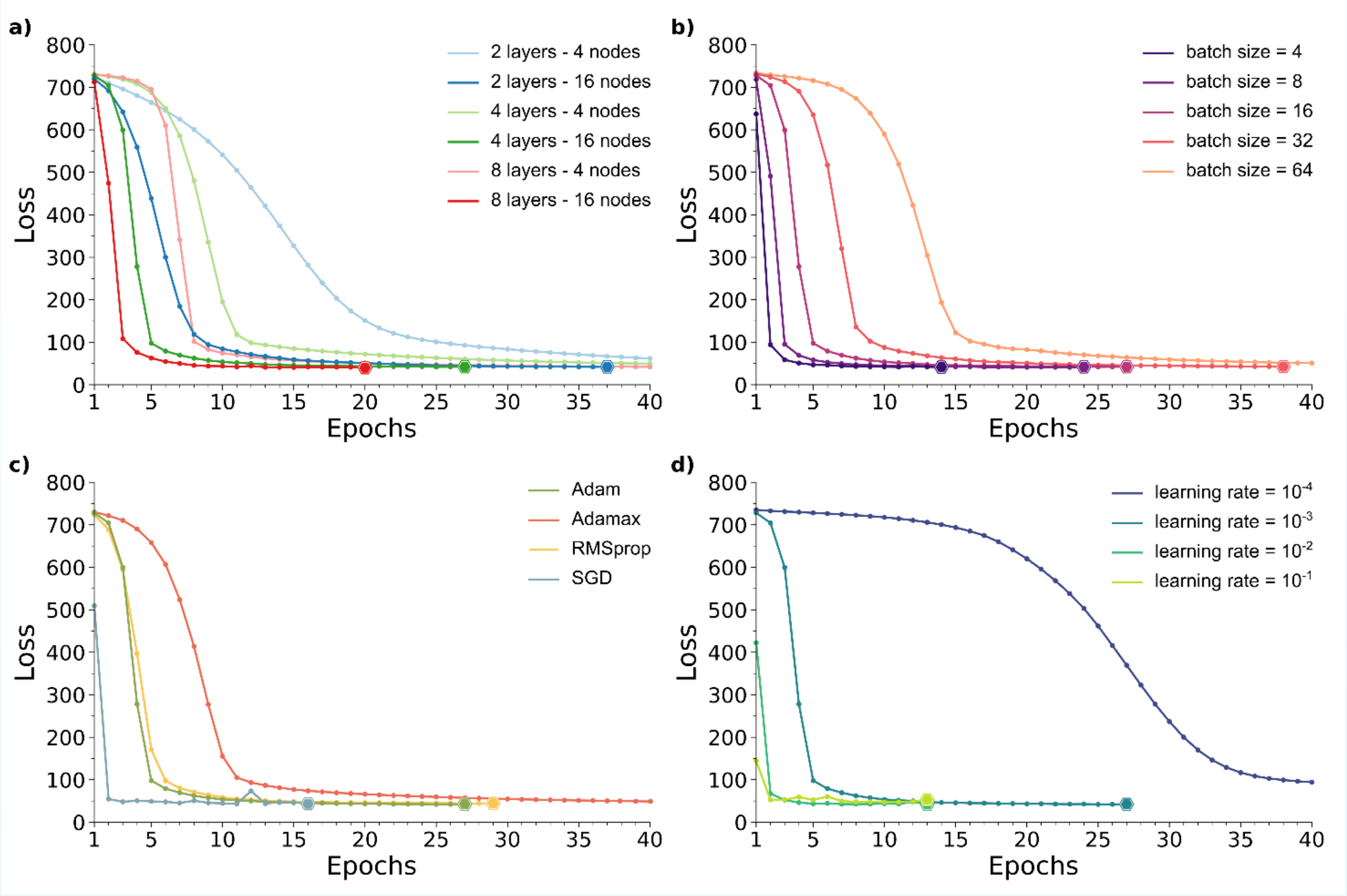

Hyperparameters tuning

Hyperparameters chosen by **trial and error**

- **Layer number** = 2 - **4** - 8
- **Layer density** = 4 - **16**
- **Optimizer** = Adadelta, Adagrad, **Adam**, Adamw, Adamax, Nadam, Adafactor, Ftrl, RMSprop and SGD
- **Batch size** = 4 – 8 – **16** – 32 - 64
- **Epoch number** = max 40
- **Learning rate** = 10^{-4} - $\mathbf{10^{-3}}$ - 10^{-2} - 10^{-1}
- **Activation function:** '**ReLU**'

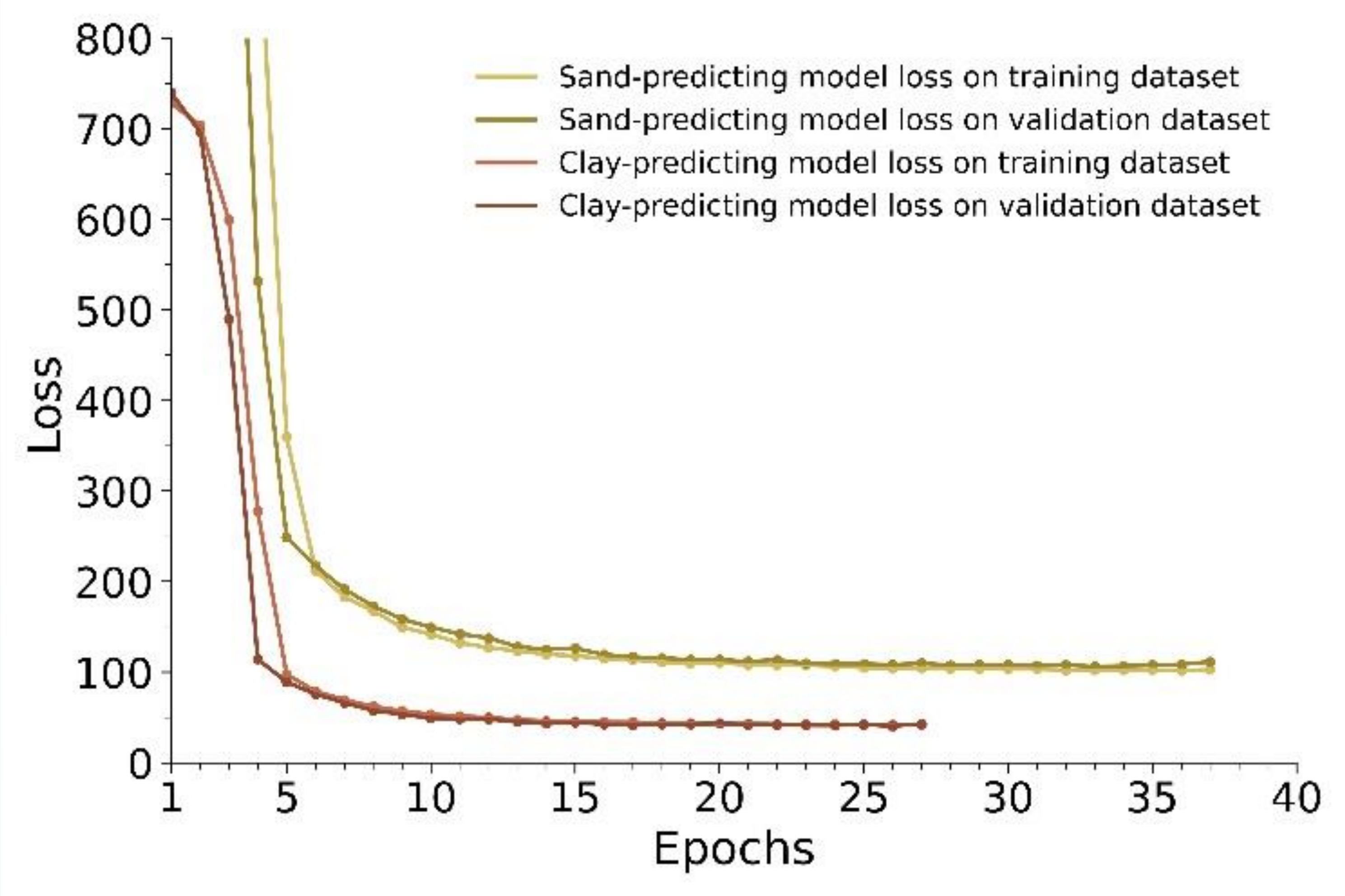

Advantages of Machine Learning

- **Higher R^2 scores** for sand and clay content predictions.
- By not being bound to a **linear relation**, ML predictions more accurately follow data in the textural triangle.
- The recent (2024) study achieves higher $\mathbf{R^2}$ showing stronger prediction accuracy. Enhanced parameter optimization improves modeling of nonlinear relationships missed in the 2022 work.
- The recent 2024 study increases resolution to **20 m x 20 m** (from 500 m x 500 m in 2022). Advanced neural networks enable finer and more accurate soil classifications.

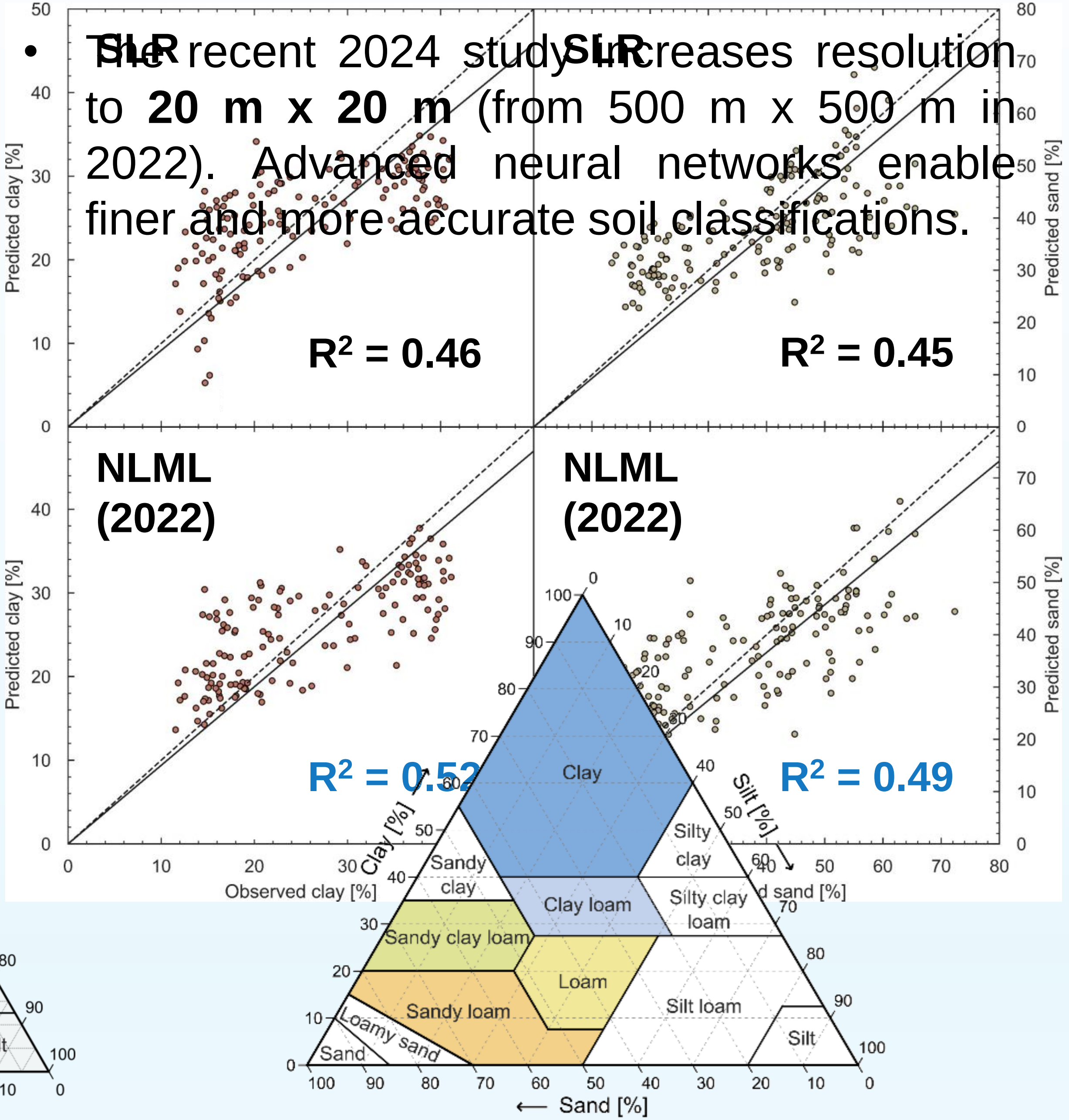

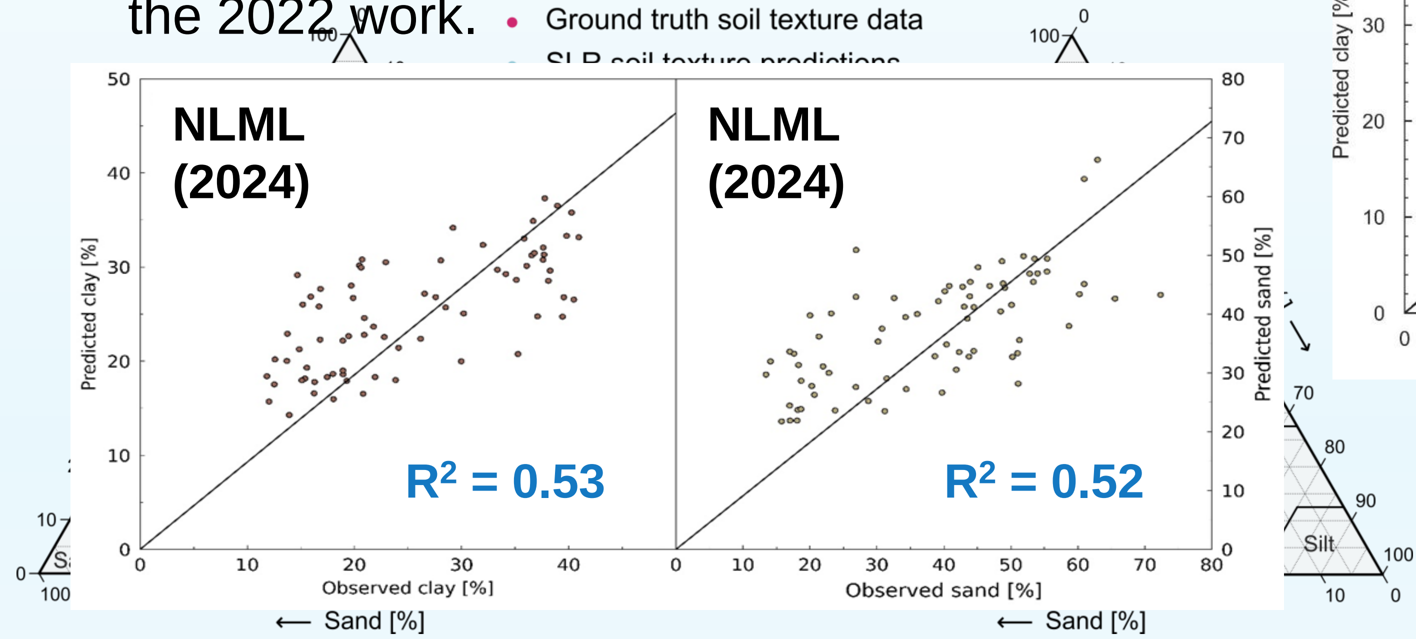

Enhancing FD detection methods

New spectral indices

GBVI and BRVI outperform GRVI, addressing shadows, glare, and man-made elements

$$\mathbf{GRVI} = \frac{\rho_G - \rho_R}{\rho_G + \rho_R}$$
(A)

$$\mathbf{GBVI} = \frac{\rho_G - \rho_B}{\rho_G + \rho_B}$$
(B)

$$\mathbf{BRVI} = \frac{\rho_B - \rho_R}{\rho_B + \rho_R}$$
(C)

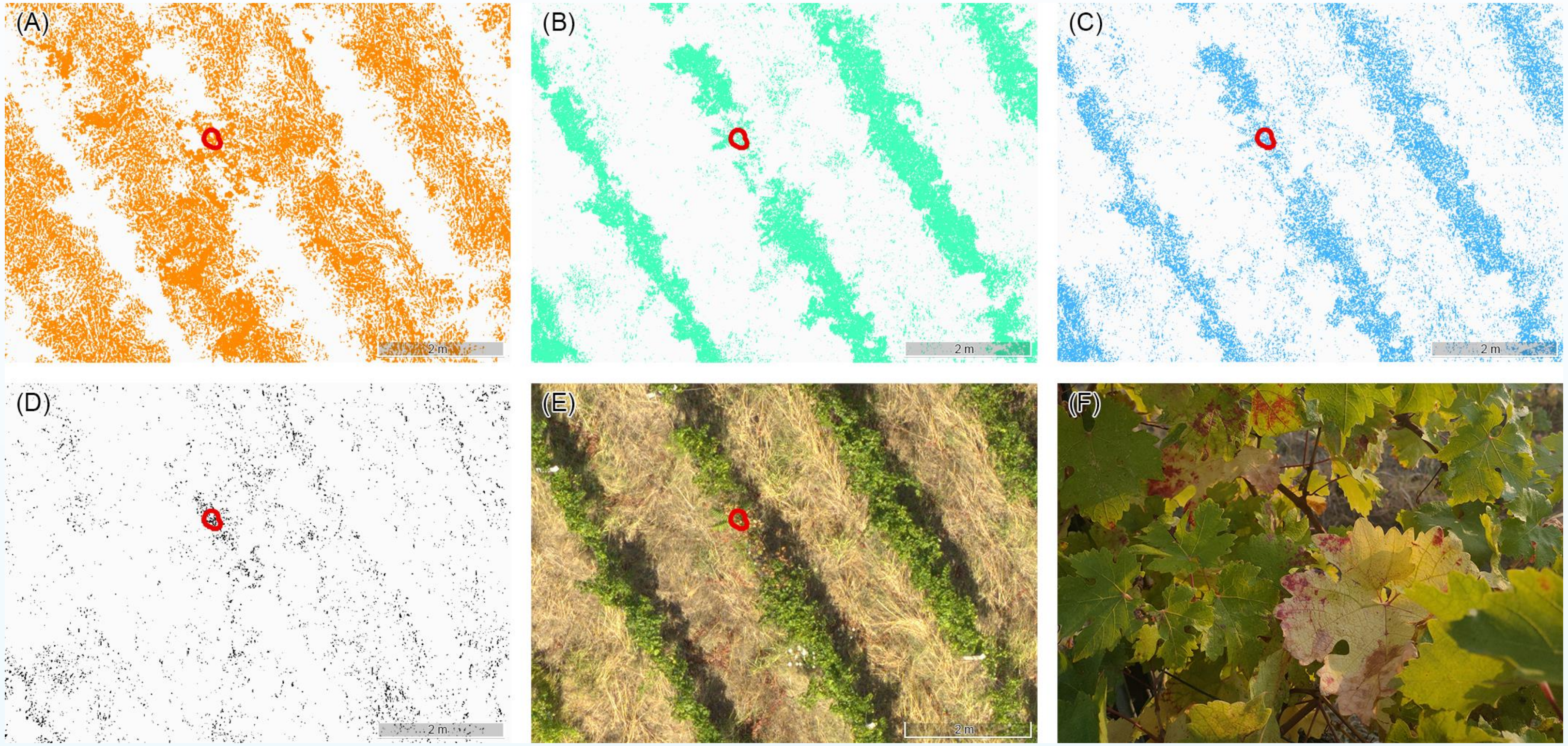

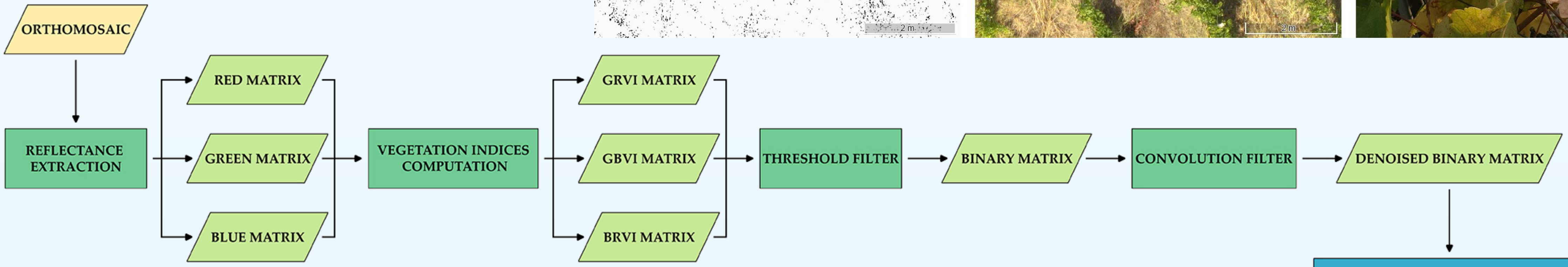

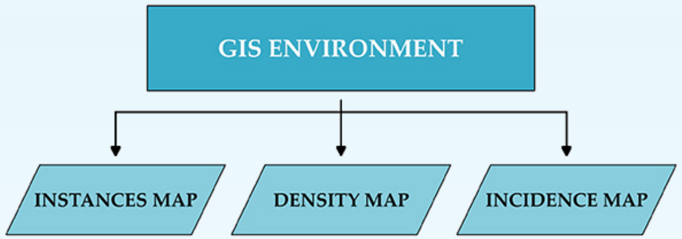

Automated pipeline

Python-based system processes RGB data, removes noise, and isolates diseased plants

Advantages of AGRS measurements

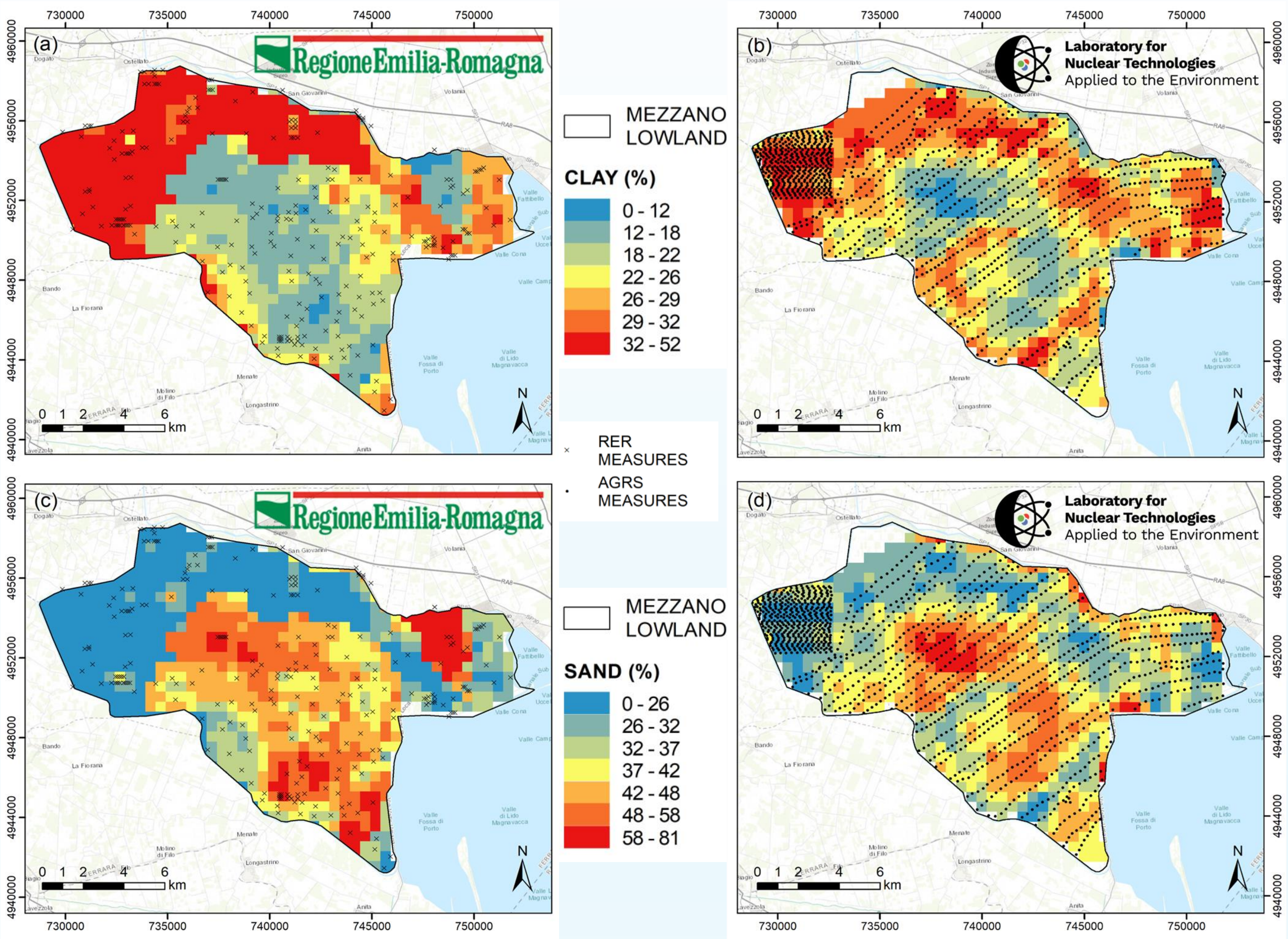

- Direct RER measurements are taken **unevenly** in the surveyed area.
- A total of **273** measurements were taken by RER.
- AGRS cover is much more **homogeneous**.
- **1469** gamma spectra were acquired, more than **5x** the amount of RER measurements.

Hydrographic interpretation of the results

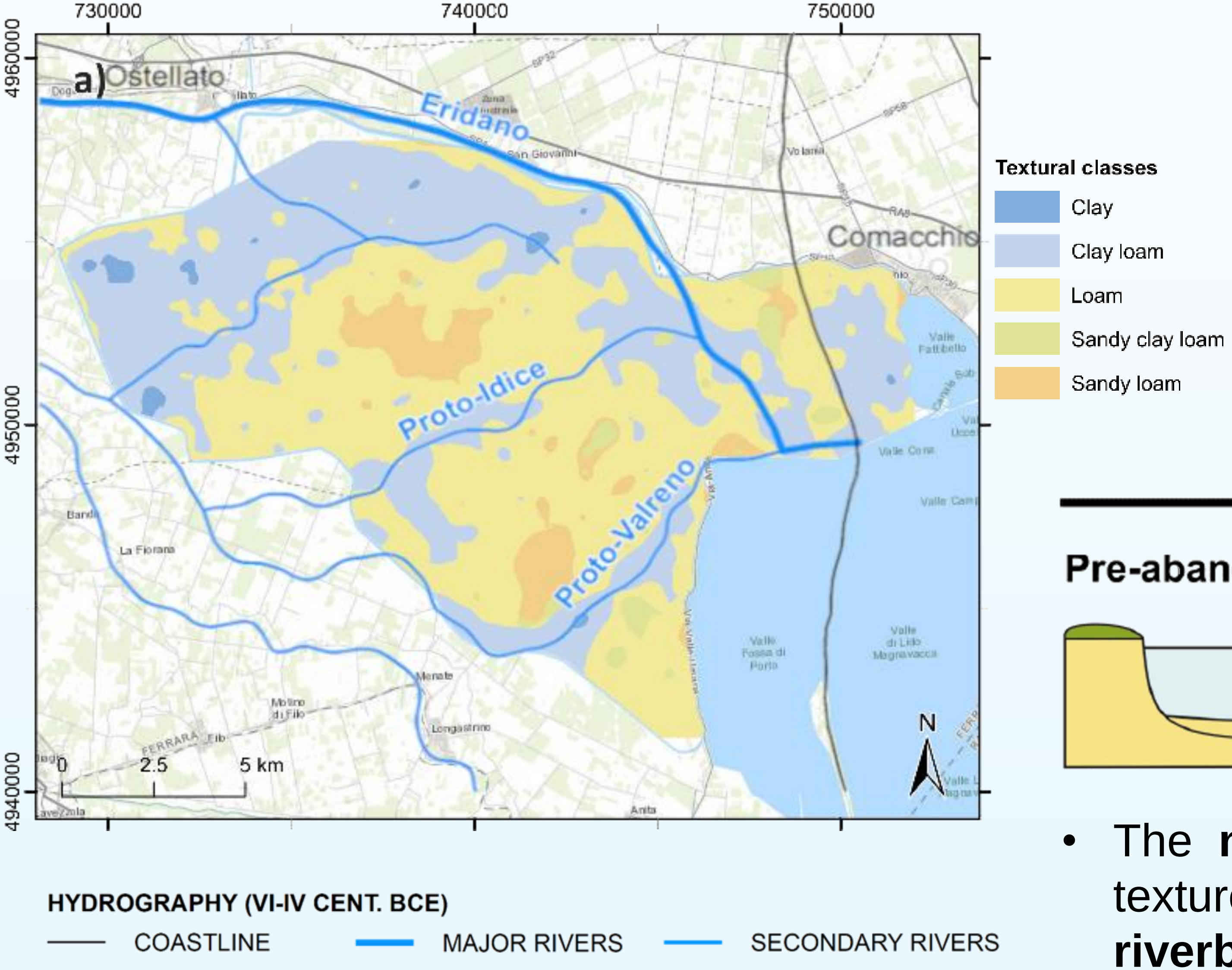

- The abandonment of the Eridano, Proto-Idice and Proto-Valreno channels led to the **sedimentary filling of their riverbeds**.
- During sedimentary filling, coarser grained particles like **sand** are deposited first, gradually followed by finer grained particles like **clay**.

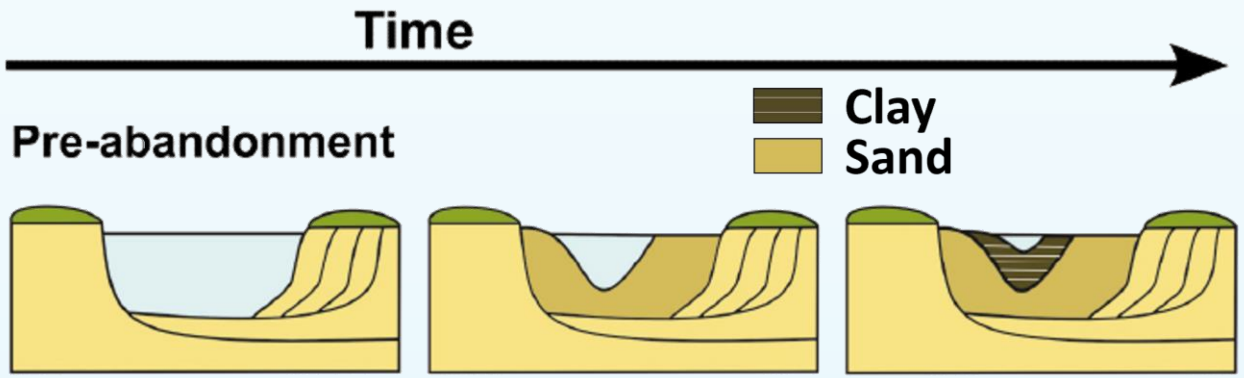

- The **narrow-shaped features** present in the soil texture prediction maps **retrace the abandoned riverbeds** of Proto-Idice and Proto-Valreno.

Spatial insights for sustainable disease management

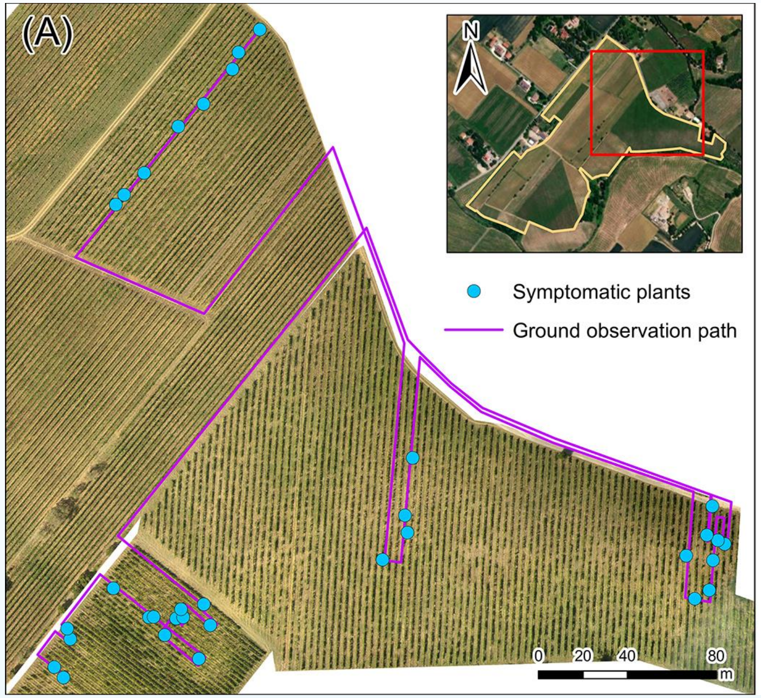

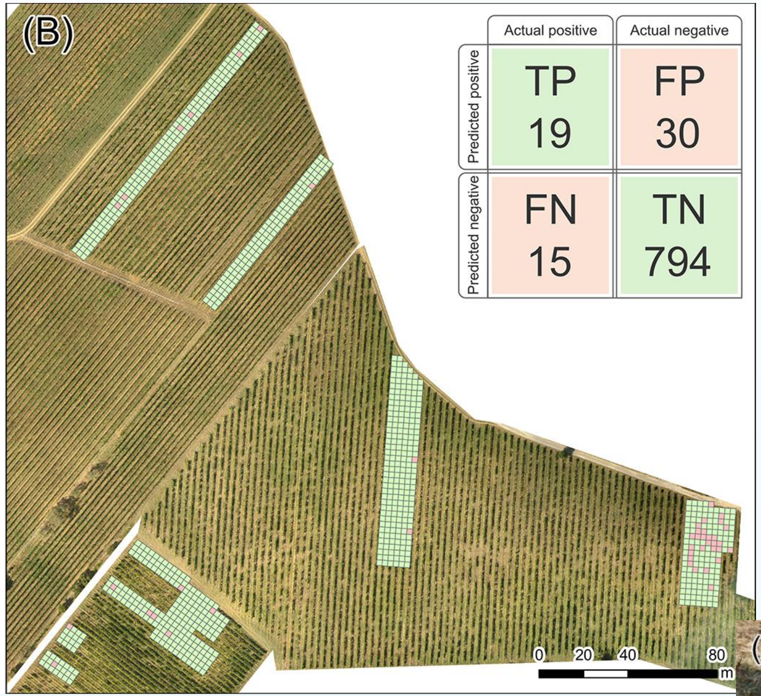

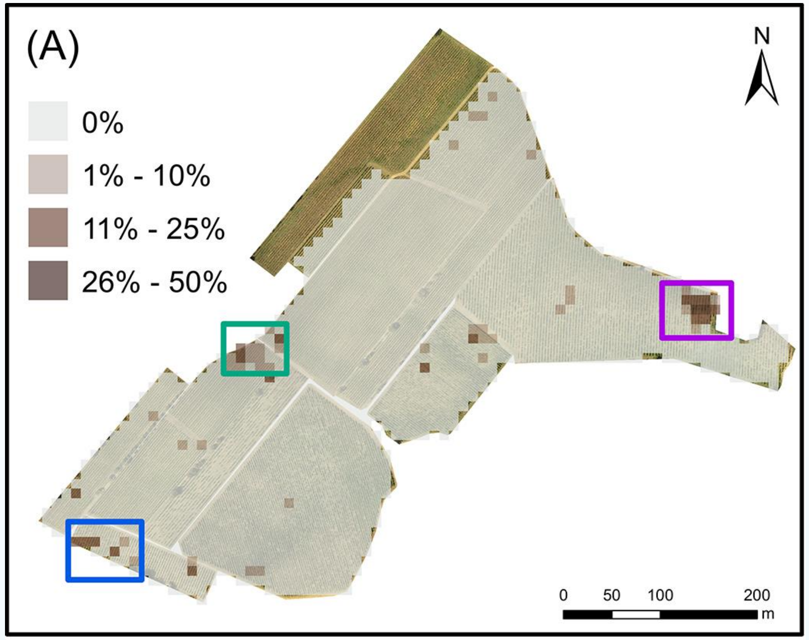

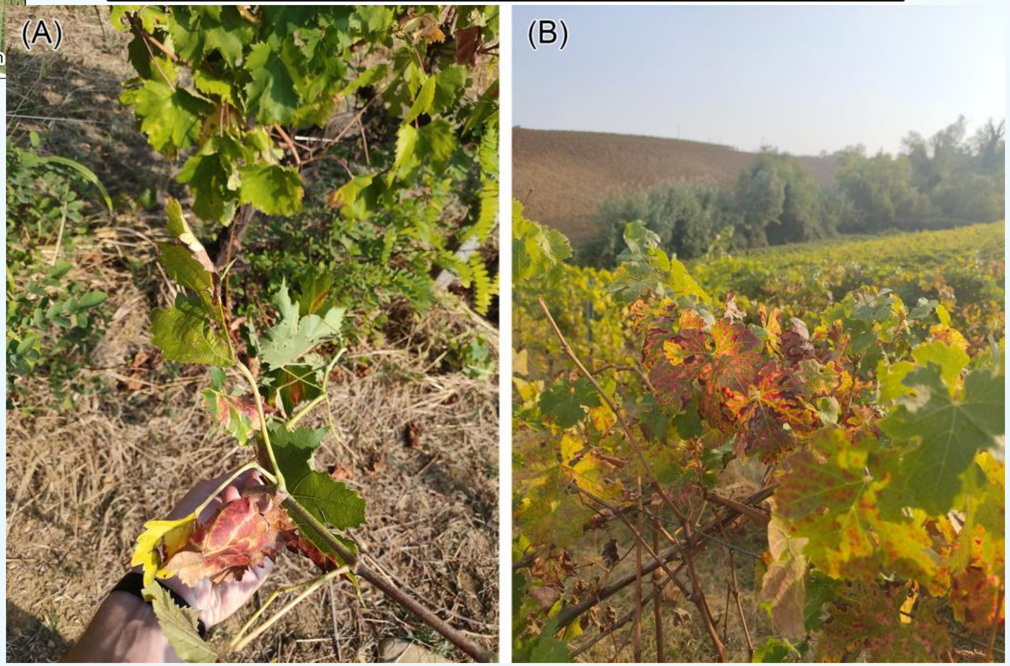

Localized risk

High-density areas (26%-50%) confined to northeast.

Sparse infections in southwest and west suggest early-stage spread.

Validation

19 true positives; high specificity (0.96).

Cautious detection ensures minimal disease oversight.

Sustainability focus

Precision mapping reduces chemicals and targets critical zones.

Supports efficient vineyard management.

Disposizione degli elettrodi - Dipolo-dipolo

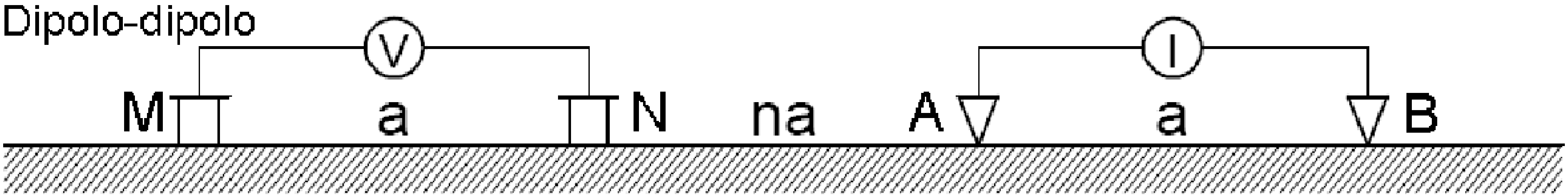

Quadripolo **Dipolo-dipolo** con disposizione assiale MN allineato con AB:

✓ MN = AB = a ; AN = na

✓ il PROFILO si ottiene spostando lungo una direzione tutti e quattro gli elettrodi contemporaneamente e si mantiene invariata la distanza intercatodica

OhmMapper - CONFIGURAZIONE

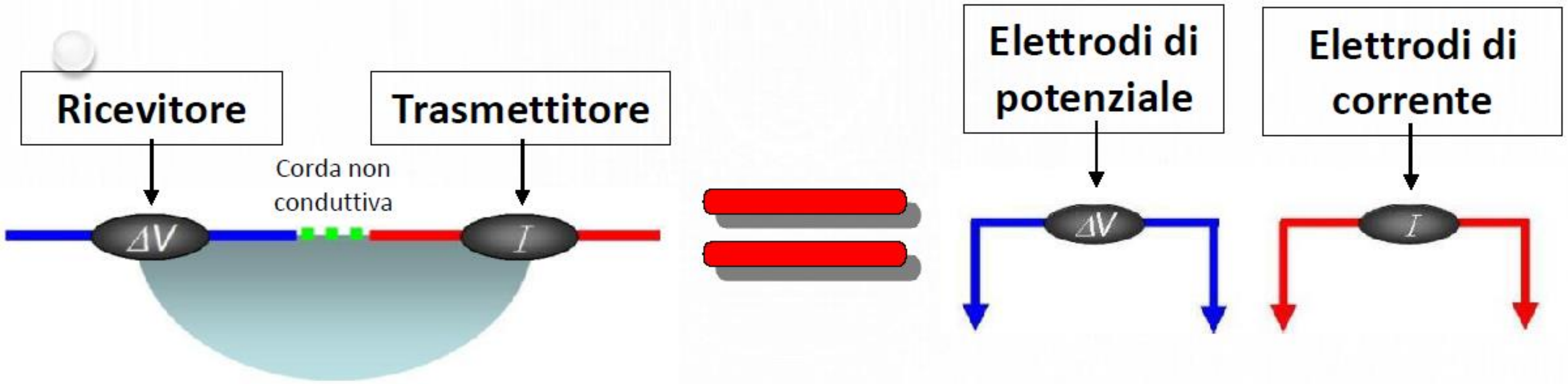

ASSIMILABILE AD UN DIPOLO-DIPOLO

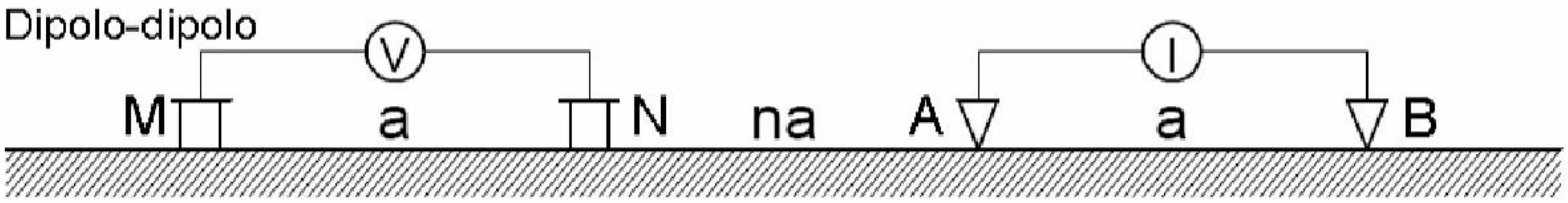

	Configurazione con antenne (*a*) da 2,5 m			Configurazione con antenne (*a*) da 5 m		
Fattore *n*	Lunghezza corda non conduttiva (*na*) [m]	Profondità indagata [m]	Lunghezza totale dello strumento [m] (con offset di 5 m)	Lunghezza corda non conduttiva (*na*) [m]	Profondità indagata [m]	Lunghezza totale dello strumento [m] (con offset di 5 m)
0,25	0,625	0,5	10,625	1,25	1	16,25
0,5	1,25	0,7	11,25	2,5	1,4	17,5
0,75	1,875	0,9	11,875	3,75	1,7	18,75
1	2,5	1	12,5	5	2	20
1,25	3,125	1,2	13,125	6,25	2,4	21,25
1,5	3,75	1,4	13,75	7,5	2,8	22,5
1,75	4,375	1,6	14,375	8,75	3,1	23,75
2	5	1,7	15	10	3,5	25
2,25	5,625	1,9	15,625	11,25	3,8	26,25
2,5	6,25	2	16,25	12,5	4,2	27,5
2,75	6,875	2,2	16,875	13,75	4,5	28,75
3	7,5	2,4	17,5	15	4,8	30
3,25	8,125	2,6	18,125	16,250	5,1	31,25
3,5	8,75	2,7	18,75	17,500	5,5	32,5
3,75	9,375	2,9	19,375	18,750	5,8	33,75
4	10	3,1	20	20	6,1	35